



A dynamical systems analysis of interacting dark energy models

V Molosi



orcid.org/0000-0001-7770-3589

Dissertation accepted in partial fulfilment of the requirements for the degree *Master of Science in Astrophysical Sciences* at the North-West University

Supervisor: Prof AA Gidelew

Graduation May 2022

32695306

Declaration

I, Vuyani Molosi (32695306), declare that this dissertation titled, "A dynamical systems analysis of interacting dark energy models" has not been submitted to this or any other university for any degree or examination, that the work presented in it is my own and that all the sources I have used or quoted have been acknowledged by complete reference.

Chapters 4 and 5 of this dissertation are based on the following publication:

- V Molosi and A Abebe, "A dynamical systems analysis of interacting dark energy models", SA Inst. Phys. Proceedings SAIP2021 (Under review).

Signed: 

Date: 07/12/2021

Abstract

We investigate using dynamical system analysis; the impacts of various interaction models whereby dark energy is coupled with dark matter. Examination on the nature of critical points for each interaction model introduced was conducted in order to obtain the cosmological consequence of each choice of interaction, with all the components of the universe considered, namely, the radiation, matter, and dark energy dominated universes. The existence of unstable radiation epoch, unstable dark matter epoch, and stable dark energy epoch will be shown for models displaying cosmologically acceptable results. Using the value of the scale factor at equality we determine the time at which the matter-dark energy equality occurred for each model. Constraints on the coupling constant b of the interacting dark energy models were placed in order to determine the phantom or quintessence behaviour of the equation of state for dark energy. We do model comparison and also compare with the Λ CDM, so as to filter our models for the best possible form of interaction term between dark matter and dark energy.

Keywords — cosmology; dark energy; dark matter; phase space; dynamical systems

CONTENTS	4
----------	---

Contents

Declaration	2
List of Figures	6
List of Tables	6
1 Introduction	8
1.1 Expanding universe	8
1.2 Dark matter	9
1.3 Dark energy	10
2 The standard cosmological model	13
2.1 The first Friedmann equation	13
2.2 Critical density and the density parameter, Ω	15
2.3 The fluid equation	16
2.4 The acceleration equation	17
2.5 Closed, open and flat universes	18
2.6 Solutions of the Friedmann equations	20
2.6.1 Matter dominated universe (non-relativistic)	20
2.6.2 Radiation dominated universe	21
2.6.3 Matter dominated universe	21
2.6.4 Dark energy dominated universe	22
2.7 Flat universe ($k=0, q = 1/2$)	22
2.7.1 Matter dominated: $P = 0, a^3\rho = Const$	22
2.7.2 Radiation dominated: $P = \frac{1}{3}\rho, a^4\rho = Const.$	23
2.7.3 Dark energy dominated: $P = -\rho, \rho = Const.$	23
2.8 Closed universe ($k=1, q > 1/2$)	23
2.8.1 Matter dominated: $P = 0, a^3\rho = Const$	24
2.8.2 Radiation dominated: $P = \frac{1}{3}\rho, a^4\rho = Const.$	25
2.8.3 Dark Energy dominated: $P = -\rho, \rho_\Lambda = \Lambda.$	25
2.9 Open universe ($k=-1, q < 1/2$)	26
2.9.1 Matter dominated: $P = 0, a^3\rho = Const$	26
2.9.2 Radiation dominated: $P = \frac{1}{3}\rho, a^4\rho = Const.$	27
2.9.3 Dark energy dominated: $P = -\rho, \rho_\Lambda = \Lambda.$	27
2.10 Solution of the Friedmann equation with total density	28
3 Dynamical systems in cosmology	31
3.1 Dynamical systems	31
3.2 Defining parameters	34

<i>CONTENTS</i>	5
3.3 Cosmological dynamical systems set up	34
4 The evolution of interacting DE models	38
4.1 Possible couplings of DM and DE	38
4.2 Trends in the studied interaction models	48
5 Interactions in the dark: constraints	51
5.1 Theoretical constraints	51
5.1.1 End of the radiation dominated epoch	51
5.1.2 End of the matter dominated epoch	53
5.1.3 End of the matter dominated epoch for different Q_s	53
5.2 Observational constraints	56
6 Discussions and conclusion	58
Acknowledgements	59
References	60

List of Figures

1	Plot showing velocity versus distance where the distances of the galaxy were determined using Cepheid variable stars. Credit: [1].	9
2	Chart showing contents of the universe, with the Planck 2018 data.	10
3	Graphic showing the timeline of the evolution of the universe. Credit: NASA/WMAP.	12
4	Possible geometries of the universe represented by the curvature index k . Credit: [2].	18
5	Evolution of the scale factor as function of time in arbitrary units for the open; flat and closed Friedmann universes.	19
6	Curve showing the scale factor as function of time for the Concordance model using the constants 2.98.	30
7	Evolution plots for the first interaction case.	40
8	Evolution plots for the interaction case B	42
9	Evolution plots for the interaction case C and D	44
10	Evolution of energy densities as a function of redshift.	49
11	Evolution of deceleration parameter and EoS are plotted as a function of redshift, for the different interactions.	50
12	Plots (a) and (b) showing the equality points for radiation-matter and matter-dark energy, respectively.	52
13	(a) shows the radiation and matter densities as function of redshift for various Q_s , while (b) shows the matter and dark energy densities as function of scale factor.	54

List of Tables

1	Combinations of eigenvalues λ_1 and λ_2 showing the stability or instability properties of an equilibrium point (x_0, y_0)	33
2	In this table we show the equality scale-factor with its corresponding equality redshift and the time at which the equality occurred, for the different models studied using initials 2.98.	55
3	In this table we present the different models that were investigated, with constraints on b^2 and DE EoS.	56
4	Constraint results on the equation of state for dark energy and matter density, $\Omega_m = 1 - \Omega_\Lambda$, from different combinations of datasets. The 2σ limits are obtained from integrals of 2.5% and 97.5% of the marginalized probability. [3].	57

5 Constraint results on the equation of state for dark energy and matter density, $\Omega_m = 1 - \Omega_\Lambda$ from individual and a combination of the datasets, at the 3σ confidence limit. [4]. 57

1 Introduction

Cosmology may be defined simply as the study of the past, present and future of the universe, or in general, just the universe as a whole. This is a well-established research field in physics which attempts to provide answers to questions like: What is the universe composed of? In spatial extent, is it finite or infinite? Is it going to come to an end at some point in the future? There are still many uncertainties that need to be investigated further by cosmologists.

1.1 Expanding universe

Observational data from Supernovae Type Ia (SNIa) [5,6], power spectrum from numerous galaxies [7] and various other sources; have proposed that our universe is currently experiencing a phase of accelerated expansion [8,9]. This expansion has caused disparities in the governing Friedmann equations and thus it is a challenging issue for standard cosmology today. One of the techniques used to determine the expansion of the universe is by calculating the Doppler effect of faraway objects. Edwin Hubble discovered through observations that galaxies move away from the earth and the velocity at which they are receding by v is proportional to the relative distance of the object d , given by the equation

$$v = H_0 d \quad (1.1)$$

which became known as the Hubble law [10], or Hubble–Lemaître law [11]. The variable H_0 is the Hubble constant where the subscript 0 denotes the value as measured today. This linear relationship is shown on figure 1 [1]. The wavelengths λ of objects that are moving towards the observer would be blue-shifted, whereas those that are moving away from the observer would be red-shifted in the spectrum. For the objects moving away from the observer, the red-shift can be given as

$$z + 1 = \frac{\lambda_0}{\lambda}. \quad (1.2)$$

Hubble presented the value of H_0 as 500 km/(sMpc), however, there have been different estimates around the value of H_0 with the improvement of data: On [5] this value is estimated to be 74.2 ± 3.6 km/(sMpc), while on [1] this value is 68 ± 2 km/(sMpc). However, in the most recent results, this value is measured to be 67.74 ± 0.46 km/(sMpc), as shown by the Planck 2018 data [12]. The Wilkinson Microwave Anisotropy Probe (WMAP) data was important in establishing the modern Standard Cosmological Model, resulting in the most precise estimate of the age of the universe of 13.75 ± 0.11 billion years [13]. Shown on figure 3 is the full timeline of the universe according to the standard model.

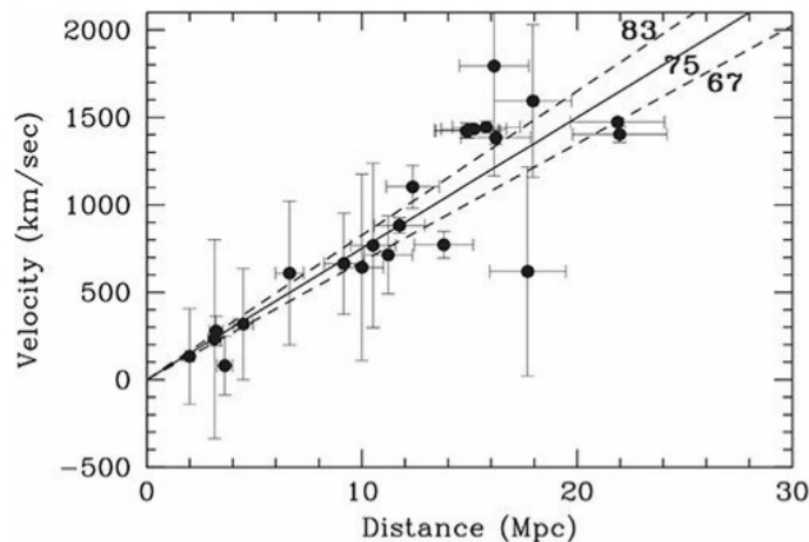


Figure 1: Plot showing velocity versus distance where the distances of the galaxy were determined using Cepheid variable stars. Credit: [1].

1.2 Dark matter

Dark matter (DM) is one component of the universe whose fundamental nature is yet to be known and as a result, over the years, cosmologists have dedicated most of their time on finding out the matter density of the universe. The matter density parameter $\Omega_{0,m}$ is crucial in determining the universe's expansion rate and spatial curvature. The content of matter of the universe is not trivial today, even if we suppose a non-zero cosmological constant, and in the recent past it was the dominant component [1].

DM has so far only been detected gravitationally, of which its candidates include black holes, massive halo objects, and many other non-baryonic particle models [14, 15]. In recent years, it has been discussed in [16], that the axion has emerged as a prominent particle candidate for providing the enigmatic dark matter in the universe. According to the Planck 2018 data, only about 4.6% of the universe is ordinary matter, while DM makes up approximately 29.5%. The rest of the content, which is approximately 65.9% is presumed to be dark energy. We illustrate on Figure 2 the numerical proportion of this content.

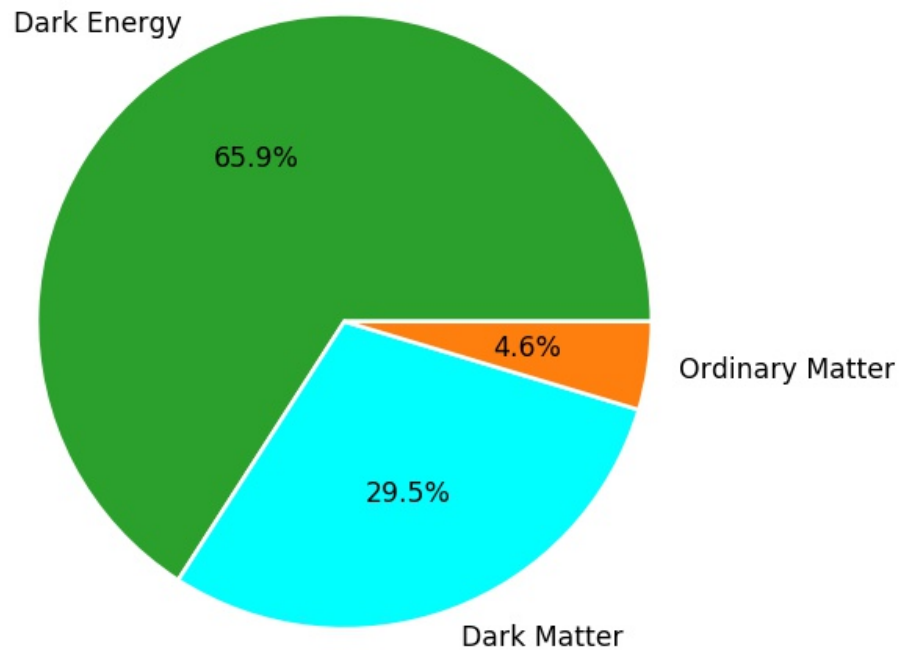


Figure 2: Chart showing contents of the universe, with the Planck 2018 data.

1.3 Dark energy

One of the most challenging unanswered topics in physics and cosmology is the existence of dark energy (DE) and the genesis of the universe's accelerating expansion [17]. The relatively recent occurrence of near-equality in the past few billion years between the densities of DE and DM, despite the fact that they must have formed differently, is a key difficulty for comprehending the rapid expansion of the universe with or without dark energy [18]. The shift from matter dominance to dark energy dominance is fast, and the fact that observational data appears to be coherent with the relatively substantial amounts of both DM and

DE suggests that we have lived through this transition phase. The cosmic coincidence problem refers to the assertion that the current era is unlikely to coincide with this quick transition phase [19].

There have been attempts to counteract the imbalances in the Friedmann equations, by either changing the governing equations or by introducing new source terms. In the framework of standard cosmology, this source is called dark energy [20]. The cosmological constant Λ , whose equation of state can be given by

$$w_\Lambda = \frac{p_\Lambda}{\rho_\Lambda} = -1, \quad (1.3)$$

is the simplest candidate for DE, which gives a vacuum energy background responsible for the current acceleration of the universe. This cosmological constant was initially introduced by Einstein and was incorporated in his general relativity field equations to keep a static universe, it was however later discovered that it itself can be considered as a component of DE that is also causing the universe's late-time acceleration.

As can be shown by 1.3, DE has a negative pressure which distinguishes it from other types of matter like radiation and baryons, which are also components of the universe. Though we know about its negative pressure, its fundamental nature is still hypothetical in modern cosmology. The value of the energy density for DE is of a very tiny magnitude, $\rho_\Lambda = \Lambda/8\pi G \approx 10^{-47} \text{ GeV}^4$. If ρ_Λ were even a fraction larger, the repulsive force would have forced the universe to expand so quickly that galaxies would not have had the time to form [21].

The cosmological constant paired with cold¹ dark² matter (CDM) gives rise to the simplest model in cosmology, known as the Λ cold dark matter, or in short, Λ CDM. According to many observations, this is the most accepted cosmological model we have today. However, the Λ CDM model does suffer from a variety of problems, such as the cosmological constant described in [22]. Understanding what dark energy is and figuring out solutions to its many related problems remains one of the most challenging issues in modern cosmology.

In the next section we will introduce and derive some of the Friedman equations and its solutions in the framework of standard cosmology.

¹*Cold* refers to the fact that DM moves slower when compared to the speed of light.

²*Dark* implies, very weak interactions with ordinary matter and electromagnetic radiation

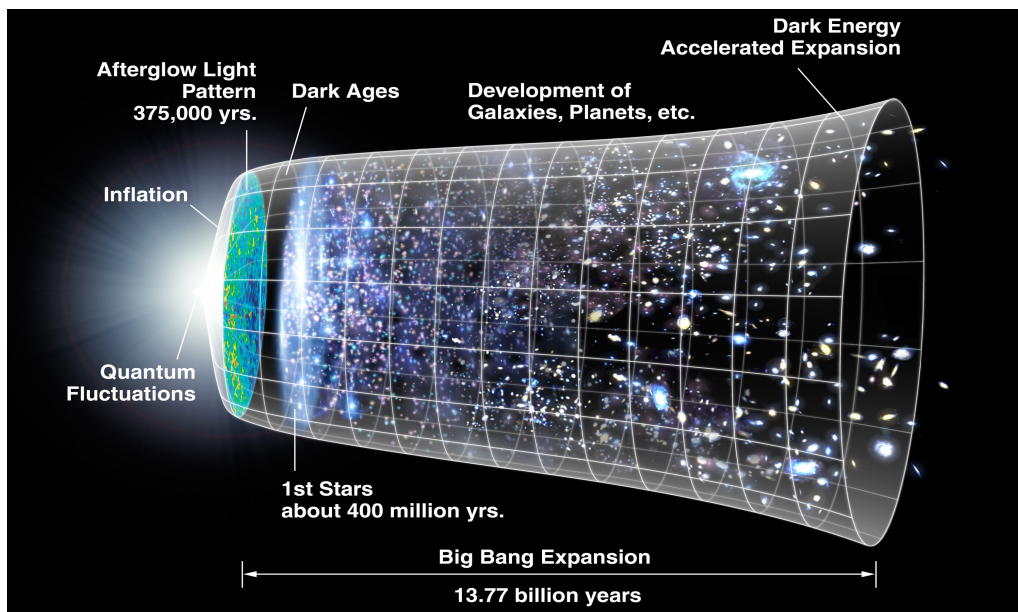


Figure 3: Graphic showing the timeline of the evolution of the universe.
Credit: [NASA/WMAP](#).

2 The standard cosmological model

The spatially flat standard cosmological model is the most widely used model in cosmology. Given the enormous success, however, several issues were discovered. Most lately, it was shown that there is a discrepancy (greater than 3σ) between the cosmological and local Hubble constant measurements [17,23]. Conventional physics, including the theory of general relativity (GR), is assumed in standard cosmology. At the expansion factor $z \sim 10^{10}$, this results in a successful account of the origin of the light elements. The production of light elements examines the relativistic relationship between expansion rate and mass density, although it is not a thorough investigation [24].

The modern standard cosmological model, sometimes referred to as the concordance model, presumes that the universe was created in the "Big Bang" from pure energy; and it is now made up of approximately 68% dark energy, 27% dark matter, and 5% of ordinary matter. While the Λ CDM model is primarily based on two theoretical models; GR and the standard model of particle physics, it also depends on other additional assumptions: (1) the universe started from a Big Bang; (2) mass energy content of the universe is made up of DE, DM, and ordinary matter; (3) GR describes the gravitational interactions between the aforementioned components; and that (4) on sufficiently large cosmic scales, the universe is homogeneous and isotropic. Regrettably, GR is considered *incomplete* in the sense that it does not explain the Big Bang cosmology, inflation, the universe's matter-antimatter imbalance, or the existence of dark energy [25]. Throughout this text, the Λ CDM model will be used as the main reference to our results, including the new information on cosmological parameters such as the one from the Planck 2018 results.

2.1 The first Friedmann equation

The equation that connects the scale factor $a(t)$, curvature constant k , curvature radius R_0 is known as the Friedman equation, named after Alexander Friedmann [1]. We begin first by deriving a non-relativistic equivalent of the Friedmann equation from Newton's law of gravity and the second law of motion. In doing so, we look at an isolated sphere with radius R_s and mass M_s in a uniform, isotropic³ expansion. From Newton's law of gravity, the gravitational force experienced by the test mass is

$$F = -\frac{GMm}{R_s^2(t)}, \quad (2.1)$$

³has the same quantity when measured in different directions

From the gravitational acceleration at the exterior of the sphere, we can work out the equation of motion for $R_s(t)$,

$$\frac{d^2 R_s}{dt^2} = -\frac{GM}{R_s^2(t)}, \quad (2.2)$$

where G is the gravitational constant, and M is the total mass. Multiplying both sides of (2.2) with dR_s/dt and integrating, we obtain the energy equation

$$\frac{1}{2} \left(\frac{dR_s}{dt} \right)^2 = \frac{GM}{R_s(t)} + U, \quad (2.3)$$

where U is just an integration constant, which we physically define as the total energy per unit mass at the surface of the expanding sphere, that is, the sum of gravitational potential energy and kinetic energy per unit mass. There are conditions that occur when U is greater than zero and when U is less than zero, when;

- $U > 0$: the right hand side of eq. (2.3) remains positive, which implies that the expanding sphere has positive total energy and will expand continuously.
- $U < 0$: the right hand side of eq. (2.3) will in the end become zero, and the sphere will have a negative total energy and will eventually collapse again.

Let us now define the radius of the sphere as follows:

$$R_s(t) = a(t)r_s, \quad (2.4)$$

where r_s is the "comoving"⁴ radius of the sphere which is equal to the physical radius at the epoch when $a(t) = 1$. Defining mass of the sphere as

$$M_s = \frac{4\pi}{3} \rho(t) R_s^3(t), \quad (2.5)$$

the energy equation then becomes

$$\frac{1}{2} r_s^2 \dot{a}^2 = \frac{4\pi}{3} G r_s^2 \rho(t) a^2(t) + U. \quad (2.6)$$

Thereafter we divide each side of eq. (5) by $r_s^2 a^2/2$ which gives the Newtonian form of the Friedmann equation;

$$\left(\frac{\dot{a}}{a} \right)^2 = \frac{8\pi G}{3} \rho(t) + \frac{2U}{r_s^2 a^2(t)}. \quad (2.7)$$

⁴Comoving distance ignores expansion of the universe, giving distance that does not vary in time.

Since $\rho(t)$ is proportional to $1/a^3(t)$, we can tell that if $U < 0$, the right hand side of eq. (2.7) will ultimately reach zero, after the expansion reverses. In General Relativity, the Friedmann equation is given as

$$\left(\frac{\dot{a}}{a}\right)^2 = \frac{8\pi G}{3}\rho(t) - \frac{kc^2}{R_0^2} \frac{1}{a^2(t)}, \quad (2.8)$$

where R_0 is the constant of the radius at present and k is the curvature index in the Friedmann-Robertson-Walker metric [1]. In this text and throughout, we have used $\rho(t)$ as the total energy density.

2.2 Critical density and the density parameter, Ω

Substituting $H(t) = \dot{a}/a$ permits us to write the Friedmann equation in terms of the Hubble parameter,

$$H(t)^2 = \frac{8\pi G}{3}\rho_c(t) - \frac{kc^2}{R_0^2} \frac{1}{a^2(t)}. \quad (2.9)$$

From the above equation we can see that space is flat ($k = 0$) when the critical density is;

$$\rho_c(t) = \frac{3H^2(t)}{8\pi G}. \quad (2.10)$$

Most often, we describe the energy density of the universe in Cosmology in terms of the density parameter Ω , which is the ratio of the total density (ρ) to the critical density (ρ_c);

$$\Omega \equiv \frac{\rho}{\rho_c} = \frac{\rho}{c^2} \frac{8\pi G}{3H^2}. \quad (2.11)$$

Substituting Ω into the Friedmann equation gives;

$$H(t)^2 = \Omega H^2(t) - \frac{kc^2}{R_0^2} \frac{1}{a^2(t)}, \quad (2.12)$$

$$\implies \Omega(t) - 1 = \frac{kc^2}{H^2(t)a^2(t)} \frac{1}{R_0^2}. \quad (2.13)$$

The right hand side of this equation 2.13 always vanishes (for the flat universe), as a result, if

- $\Omega = 1$, then it will be 1 at all times.

In other cases, the value of Ω varies with time, but if

- $\Omega > 1$, then it will always be greater than unity;
- $\Omega < 1$, then it will always be less than unity because the sign on the right hand side cannot change [1].

2.3 The fluid equation

Consider the first law of thermodynamics also known as the law of conservation of energy,

$$dE = -PdV + dQ, \quad (2.14)$$

where dE is the internal energy of a volume of a fluid, PdV is work and dQ is the heat. As the Universe is assumed to be homogeneous, its expansion is *adiabatic*⁵, therefore:

$$dE + PdV = 0 \implies \dot{E} + P\dot{V} = 0. \quad (2.15)$$

For a sphere of comoving radius r_s we have

$$V = \frac{4\pi}{3} r_s^3 a^3(t), \quad (2.16)$$

and its derivative is

$$\dot{V} = \frac{4\pi}{3} r_s^3 (3a^2(t) \dot{a}) = V \left(3 \frac{\dot{a}}{a} \right). \quad (2.17)$$

Introducing the total energy density ρ , we have the internal energy of the sphere as

$$E = V\rho c^2,$$

while the rate of change of the internal energy being

$$\dot{E} = (V\dot{\rho} + \dot{V}\rho)c^2. \quad (2.18)$$

Using equations 2.15, 2.17 and 2.18 we end up with

$$V \left(\dot{\rho} + 3 \frac{\dot{a}}{a} \rho + 3 \frac{\dot{a}}{a} \frac{P}{c^2} \right) = 0, \quad (2.19)$$

hence,

$$\dot{\rho} + 3 \frac{\dot{a}}{a} \left(\rho + \frac{P}{c^2} \right) = 0. \quad (2.20)$$

Equation (2.20) is the fluid equation, sometimes referred to as the "continuity equation", which describes the evolution of energy density in an expanding universe [1,26].

⁵a process that occurs without the transfer of heat.

In solving the fluid equation, we require an additional equation of state that relates ρ and P . Assume we write this equation as $P = w\rho$, where w could change with time, but we will suppose its time derivatives are trivial compared to time derivatives of the density ρ . The fluid equation then implies,

$$\frac{\dot{\rho}}{\rho} = -3(1+w)\frac{\dot{a}}{a}, \quad (2.21)$$

$$\implies \ln\left(\frac{\rho}{\rho_0}\right) = -3(1+w)\ln\left(\frac{a}{a_0}\right), \quad (2.22)$$

hence,

$$\frac{\rho}{\rho_0} = \left(\frac{a}{a_0}\right)^{-3(1+w)}, \quad (2.23)$$

is the solution of the fluid equation.

2.4 The acceleration equation

To derive the acceleration equation, we multiply eq. (2.9) by a^2 ;

$$\dot{a}^2 = \frac{8\pi G}{3}\rho(t)a^2 - \frac{kc^2}{R_0^2}. \quad (2.24)$$

The time derivative yields;

$$2\dot{a}\ddot{a} = \frac{8\pi G}{3}(\dot{\rho}a^2 + 2\rho a\dot{a}). \quad (2.25)$$

Dividing both sides of eq. (17) by $2\dot{a}a$ we get

$$\frac{\ddot{a}}{a} = \frac{4\pi G}{3}\left(\dot{\rho}\frac{a}{\dot{a}} + 2\rho\right). \quad (2.26)$$

From the fluid equation 2.20, substituting

$$\dot{\rho}\frac{a}{\dot{a}} = -3\left(\rho + \frac{P}{c^2}\right), \quad (2.27)$$

we obtain

$$\frac{\ddot{a}}{a} = -\frac{4\pi G}{3}\left(\rho + 3\frac{P}{c^2}\right). \quad (2.28)$$

From 2.28 we see that if $\rho, P > 0$, the expansion of the universe decelerates. A higher P causes stronger deceleration for a given ρ , for instance, a radiation dominated universe decelerates faster than a matter dominated universe.

2.5 Closed, open and flat universes

The constant k , which represents the spatial curvature of the universe, actually holds a significant meaning within general relativity. To best describe the geometry of the universe, we rewrite the Friedmann equation as:

$$\frac{1}{2}\dot{a}^2 + V_{\text{eff}}(a) = -\frac{1}{2}k, \quad (2.29)$$

where $V_{\text{eff}}(a) = -((4\pi G)/3)\rho a^2$ is the effective potential. There are then three possible geometries of the universe that we can describe using the curvature index:

- $k > 0$ (closed universe), indicating a negative energy; and the trajectories are bounded, meaning that the universe will expand up to a point in which the expansion will eventually reverse and the universe contracts. This is an elliptic surface and thus the sum of angles of the triangle on this surface would be greater than 180° .
- $k < 0$ (open universe), implies that the energy is positive and the trajectories are unbounded, meaning that the universe will expand forever. As figure 4 [2] shows, this is a hyperbolic surface and so the sum of angles of the triangle would be less than 180° .
- $k = 0$, a flat universe. On a plane surface, the sum of the triangle angles sums up to 180° .

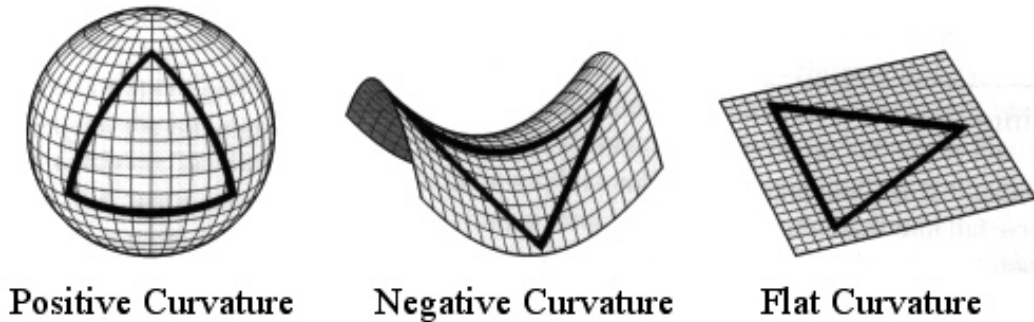


Figure 4: Possible geometries of the universe represented by the curvature index k . Credit: [2].

On figure 5 the evolution of the scale factor as function of time for a closed, flat and open universe is indicated. A **closed universe** means that expansion will

be stopped by gravity, causing it to contract, which would result in a massive contraction of the universe in what we call a "big crunch", from which it could begin again. The density of the universe would have to be greater than the critical density $\rho > \rho_c$.

On the other hand, an **open universe** means that gravity would be too weak to stop the expansion, meaning it would expand forever. The density of the universe would be less than the critical density $\rho < \rho_c$. For a **flat universe**, the density is equal to the critical value; consequently the universe will only start to contract after an infinite amount of time. [27].

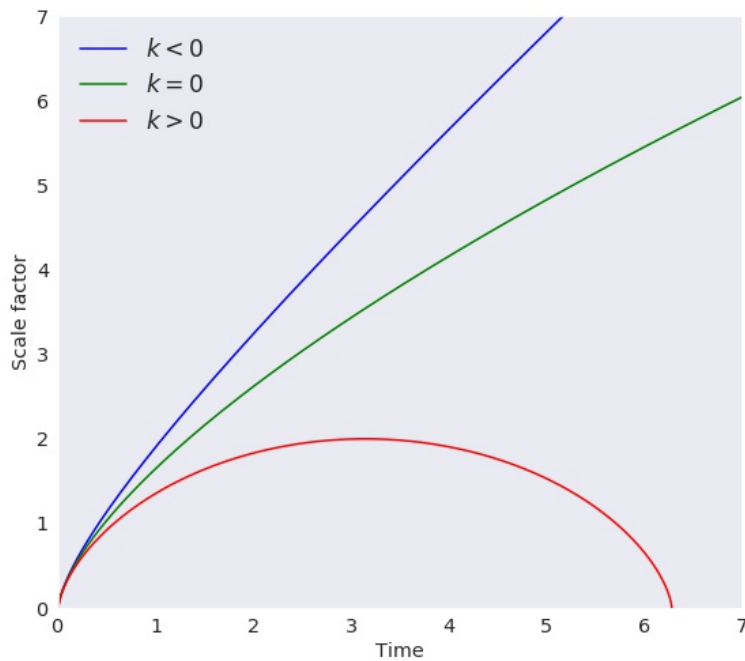


Figure 5: Evolution of the scale factor as function of time in arbitrary units for the open; flat and closed Friedmann universes.

2.6 Solutions of the Friedmann equations

From the definition of the Hubble rate, $H = \frac{\dot{a}}{a}$, we have that

$$\dot{H} = \frac{\ddot{a}}{a} - H^2 = -H^2 \left(1 - \frac{\ddot{a}}{H^2 a} \right) \equiv -H^2(1 + q), \quad (2.30)$$

where we define the deceleration parameter q as:

$$q \equiv -\frac{\ddot{a}}{H^2 a}. \quad (2.31)$$

2.6.1 Matter dominated universe (non-relativistic)

We model matter-dominated universe by *dust approximation*⁶, $P = 0$. We then have, from the acceleration equation,

$$\frac{\ddot{a}}{a} + \frac{4\pi G}{3c^2} \rho = 0. \quad (2.32)$$

Re-writing in terms of H , we have,

$$-H^2 q + \frac{4\pi G}{3c^2} \rho = 0, \quad (2.33)$$

thus, we get and define the density of the universe ρ

$$\rho \equiv \frac{3H^2}{4\pi G} q. \quad (2.34)$$

Noting that the value q gives the relationship between the density of the universe ρ and the critical density ρ_c as

$$q = \frac{\rho}{2\rho_c}, \quad (2.35)$$

the first Friedmann equation becomes

$$H^2 - 2H^2 q = -\frac{k}{a^2}, \quad (2.36)$$

$$\implies -k = a^2 H^2 (1 - 2q). \quad (2.37)$$

⁶Dust approximation for a matter-dominated universe means that the matter is approximated as stationary dust particles which produce no pressure — $P = 0$.

Since both the scale factor a and the Hubble parameter H cannot be zero, the spatial curvature constant k takes the values

$$k = \begin{cases} +1 & \text{closed universe} \\ 0 & \text{flat universe} \\ -1 & \text{open universe} \end{cases} \quad (2.38)$$

and for the deceleration parameter we have $q = 1/2$ for flat universe, $q > 1/2$ for closed universe and lastly $q < 1/2$ for the open universe.

2.6.2 Radiation dominated universe

Radiation dominated Universe is modelled by perfect fluid approximation where $P = \frac{1}{3}\rho$. The second Friedmann equation then yields,

$$\dot{\rho}_r + 3\frac{\dot{a}}{a}(\rho_r + \frac{1}{3}\rho_r) = \dot{\rho}_r + 4\frac{\dot{a}}{a}\rho_r = 0; \quad (2.39)$$

and thereafter multiplying by a^4 we obtain,

$$a^4\dot{\rho}_r + 4\dot{a}a^3\rho_r = 0 \implies \frac{d}{dt}(a^4\rho_r) = 0 \implies a^4\rho_r = a_0^4\rho_0 = \text{Const}, \quad (2.40)$$

$$\therefore \rho_r(t) = \rho_{0,r} \frac{a_0^4}{a^4(t)}. \quad (2.41)$$

2.6.3 Matter dominated universe

The second Friedmann equation becomes;

$$\dot{\rho}_m + 3\frac{\dot{a}}{a}\rho_m = 0, \quad (2.42)$$

and multiplying both sides by a^3 to get,

$$a^3\dot{\rho}_m + 3\dot{a}a^2\rho_m = 0, \quad (2.43)$$

$$\implies \frac{d}{dt}(a^3\rho_m) = 0, \quad (2.44)$$

$$a^3\rho_m = a_0^3\rho_0 = \text{Const}, \quad (2.45)$$

$$\therefore \rho_m(t) = \rho_{0,m} \frac{a_0^3}{a^3(t)}. \quad (2.46)$$

2.6.4 Dark energy dominated universe

For dark energy, the equation of state is $P = -\rho$, then by the fluid equation we have

$$\begin{aligned} \dot{\rho} + 3\frac{\dot{a}}{a}(\rho + P) &= \dot{\rho} + 3\frac{\dot{a}}{a}(\rho - \rho) = 0, \\ \dot{\rho} &= 0, \end{aligned} \quad (2.47)$$

where we have set $c = 1$ for the speed of light. Thus for dark energy;

$$\rho_{\Lambda} = \Lambda = \text{Const.} \quad (2.48)$$

2.7 Flat universe ($k=0$, $q = 1/2$)

We derive the solutions of the Friedmann equation when $k = 0$.

2.7.1 Matter dominated: $P = 0$, $a^3\rho = \text{Const}$

$$a^3\rho = a_0^3\rho_0 \implies \rho = \left(\frac{a_0}{a}\right)^3 \rho_0.$$

From the first Friedmann equation we have;

$$\frac{\dot{a}^2}{a^2} = \frac{8\pi G}{3}\rho_0\left(\frac{a_0}{a}\right)^3, \quad (2.49)$$

$$\implies \frac{da}{dt} = \sqrt{\frac{8\pi G}{3}\rho_0\left(\frac{a_0^3}{a}\right)}. \quad (2.50)$$

At the time of the Big Bang ($t = 0$), we get that $a(t = 0) = 0$. Assuming the convention that $a_0 = 1$ and applying the assumption that the universe is flat, $\rho_0 = \rho_c$, we thus have

$$a(t) = \frac{3}{2}\left(\frac{8\pi G\rho_0}{3}\right)^{1/3} t^{2/3} = \left(6\pi G\rho_c\right)^{1/3} t^{2/3}; \quad (2.51)$$

and substituting $\rho_c = 3H_0^2/8\pi G$, we get

$$a(t) = \left(\frac{3}{2}H_0^2\right)^{2/3} t^{2/3}. \quad (2.52)$$

2.7.2 Radiation dominated: $P = \frac{1}{3}\rho$, $a^4\rho = \text{Const.}$

From the first Friedmann equation we obtain

$$\frac{\dot{a}^2}{a^2} = \frac{8\pi G}{3}\rho_0\left(\frac{a_0}{a}\right)^4, \quad (2.53)$$

$$\implies \frac{da}{dt} = \sqrt{\frac{8\pi G}{3}\rho_0\left(\frac{a_0^4}{a}\right)}. \quad (2.54)$$

Looking at the same initial conditions at Big Bang ($t = 0$) with $a_0 = 1$, we have that $a(0) = 0$, thus

$$a(t) = \left(\frac{32\pi G\rho_0}{3}\right)^{1/4} t^{1/2} = \left(\frac{32\pi G\rho_c}{3}\right)^{1/4} t^{1/2}, \quad (2.55)$$

and substituting ρ_c , we then end up with

$$a(t) = \left(2H_0\right)^{1/2} t^{1/2}. \quad (2.56)$$

2.7.3 Dark energy dominated: $P = -\rho$, $\rho = \text{Const.}$

Since $k = 0$, according to equation 2.8, we have,

$$\left(\frac{\dot{a}}{a}\right)^2 = \frac{8\pi G}{3}\Lambda, \quad (2.57)$$

$$\implies \frac{1}{a}da = \left(\sqrt{\frac{8\pi G}{3}\Lambda}\right)dt, \quad (2.58)$$

hence,

$$a(t) = a_0 \exp\left(t\sqrt{\frac{8\pi G}{3}\Lambda}\right). \quad (2.59)$$

As the scale factor 2.59 is exponential in this case, it implies that the universe will expand forever, as it is free from the singularity, or collapsing into a "Big Crunch".

2.8 Closed universe ($k=1$, $q > 1/2$)

We derive the solutions of the Friedmann equation when $k = 1$.

2.8.1 Matter dominated: $P = 0, a^3\rho = \text{Const}$

From 2.8 we now obtain,

$$\frac{\dot{a}^2}{a^2} = \frac{8\pi G}{3}\rho_0\left(\frac{a_0}{a}\right)^3 - \frac{1}{a^2}, \quad (2.60)$$

$$\implies \frac{da}{dt} = \sqrt{\frac{8\pi G\rho_0 a_0^3}{3a} - 1}. \quad (2.61)$$

We now introduce the "arc-parameter measure of time" also called "conformal time" given as

$$d\eta \equiv \frac{dt}{a(t)},$$

and defining a new constant A as,

$$A \equiv \frac{4\pi G\rho_0}{3} = H_0^2 q_0 = \frac{q_0}{2q_0 - 1},$$

where we have used equations 2.37 and the fact that $a_0 = 1$ today. This then results in;

$$\eta - \eta_0 = \int_0^a \frac{1}{\sqrt{2A\tilde{a} - \tilde{a}^2}} d\tilde{a} = \arcsin\left(\frac{a - A}{A}\right) + \frac{1}{2}\pi. \quad (2.62)$$

We require that $\eta = 0$ at $a = 0$ which means that $\eta_0 = 0$, hence

$$\frac{a - A}{A} = \sin\left(\eta - \frac{1}{2}\pi\right) = -\cos(\eta) \implies a = A(1 - \cos(\eta)). \quad (2.63)$$

Since $dt = ad\eta$, we have

$$t - t_0 = \int ad\eta = \int A(1 - \cos(\eta))d\eta = A(\eta - \sin(\eta)). \quad (2.64)$$

At $t = 0$ we want $\eta = 0$ which implies $t_0 = 0$ and thus finally we can express the scale factor a in terms of the conformal time η :

$$a = \frac{q_0}{2q_0 - 1}(1 - \cos(\eta)), \quad (2.65)$$

$$t = \frac{q_0}{2q_0 - 1}(\eta - \sin(\eta)).$$

2.8.2 Radiation dominated: $P = \frac{1}{3}\rho, a^4\rho = \text{Const.}$

The first Friedmann equation yields,

$$\frac{\dot{a}^2}{a^2} = \frac{8\pi G}{3}\rho_0\left(\frac{a_0}{a}\right)^4 - \frac{1}{a^2}, \quad (2.66)$$

$$\implies \frac{da}{dt} = \sqrt{\frac{8\pi G\rho_0 a_0^4}{3a^2} - 1}. \quad (2.67)$$

Once again defining a new constant $A_1 \equiv \frac{8\pi G\rho_0}{3} = \frac{2q_0}{2q_0-1}$ thus,

$$\eta - \eta_0 = \int_0^a \frac{1}{\sqrt{A_1 - \tilde{a}^2}} d\tilde{a} = \arcsin\left(\frac{a}{\sqrt{A_1}}\right). \quad (2.68)$$

With the condition $\eta = 0$ at $t = 0$ sets $t_0 = \sqrt{A_1}$, and hence

$$a = \sqrt{\frac{2q_0}{2q_0-1}} \sin(\eta), \quad (2.69)$$

$$t = \sqrt{\frac{2q_0}{2q_0-1}} (1 - \cos(\eta)).$$

2.8.3 Dark Energy dominated: $P = -\rho, \rho_\Lambda = \Lambda.$

The Friedmann equation 2.8 implies,

$$\left(\frac{\dot{a}}{a}\right)^2 = \frac{8\pi G}{3}\rho_\Lambda - \frac{1}{a^2} \quad (2.70)$$

$$\implies \dot{a} = \sqrt{\left(\frac{8\pi G}{3}\Lambda\right)a^2 - 1}. \quad (2.71)$$

By letting the constant B be defined as

$$B \equiv \sqrt{\frac{8\pi G}{3}\Lambda},$$

we end up with

$$B^{-1/2} \sinh^{-1}(B^{1/2}a) = t, \quad (2.72)$$

thus,

$$a(t) = B^{-1/2} \sinh(B^{1/2}t). \quad (2.73)$$

2.9 Open universe ($k = -1$, $q < 1/2$)

2.9.1 Matter dominated: $P = 0$, $a^3\rho = \text{Const}$

From the Friedmann equation 2.8,

$$\frac{\dot{a}^2}{a^2} = \frac{8\pi G}{3}\rho_0\left(\frac{a_0}{a}\right)^3 + \frac{1}{a^2}, \quad (2.74)$$

$$\implies \frac{da}{dt} = \sqrt{\frac{8\pi G\rho_0 a_0^3}{3a} + 1}. \quad (2.75)$$

Allowing that $a_0 = 0$ and defining \tilde{A} as $\tilde{A} \equiv \frac{4\pi G\rho_0}{3} = \frac{q_0}{2q_0-1}$, it then follows that

$$\eta - \eta_0 = \int_0^a \frac{1}{\sqrt{2\tilde{A}\tilde{a} + \tilde{a}^2}} d\tilde{a} = \ln\left(\frac{a + \tilde{A} + \sqrt{a(2\tilde{A} + A)}}{\tilde{A}}\right), \quad (2.76)$$

$$\implies \eta - \eta_0 = \cosh^{-1}\left(\frac{a}{\tilde{A}} + 1\right). \quad (2.77)$$

Likewise, we require that $\eta = 0$ at $a = 0$ which means that $\eta_0 = 0$, hence

$$\frac{a + \tilde{A}}{\tilde{A}} = \cosh(\eta) \implies a = \tilde{A}(\cosh(\eta) - 1). \quad (2.78)$$

Since $dt = ad\eta$, we have

$$t - t_0 = \int ad\eta = \int \tilde{A}(\cosh(\eta) - 1)d\eta = \tilde{A}(\sinh(\eta) - \eta). \quad (2.79)$$

At $t = 0$ we want $\eta = 0$ which implies $t_0 = 0$ and thus finally we can express the scale factor a in terms of the conformal time η ,

$$a = \frac{q_0}{2q_0 - 1}(\cosh(\eta) - 1), \quad (2.80)$$

$$t = \frac{q_0}{2q_0 - 1}(\sinh(\eta) - \eta).$$

2.9.2 Radiation dominated: $P = \frac{1}{3}\rho$, $a^4\rho = \text{Const.}$

The first Friedmann equation 2.8 yields

$$\frac{\dot{a}^2}{a^2} = \frac{8\pi G}{3}\rho_0\left(\frac{a_0}{a}\right)^4 + \frac{1}{a^2}, \quad (2.81)$$

$$\implies \frac{da}{dt} = \sqrt{\frac{8\pi G\rho_0 a_0^4}{3a^2} + 1}. \quad (2.82)$$

Once again defining a new constant $\tilde{A}_1 \equiv \frac{8\pi G\rho_0}{3} = \frac{2q_0}{2q_0-1}$ then,

$$\eta - \eta_0 = \int_0^a \frac{1}{\sqrt{\tilde{A}_1 + \tilde{a}^2}} d\tilde{a} = \sinh^{-1}\left(\frac{a}{\sqrt{\tilde{A}_1}}\right). \quad (2.83)$$

Given the condition $\eta = 0$ at $t = 0$ setting $t_0 = \sqrt{\tilde{A}_1}$ we end up with

$$a = \sqrt{\frac{2q_0}{2q_0-1}} \sinh(\eta), \quad (2.84)$$

and

$$t = \sqrt{\frac{2q_0}{2q_0-1}} (\cosh(\eta) - 1). \quad (2.85)$$

2.9.3 Dark energy dominated: $P = -\rho$, $\rho_\Lambda = \Lambda$.

The equation 2.8 implies

$$\left(\frac{\dot{a}}{a}\right)^2 = \frac{8\pi G}{3}\rho_\Lambda + \frac{1}{a^2}, \quad (2.86)$$

$$\implies \dot{a} = \sqrt{\left(\frac{8\pi G}{3}\Lambda\right)a^2 + 1}. \quad (2.87)$$

Therefore the constant \tilde{B} is defined as

$$\tilde{B} \equiv \sqrt{\frac{8\pi G}{3}\Lambda},$$

then

$$\tilde{B}^{-1/2} \sinh^{-1}\left(\tilde{B}^{1/2}a\right) = t, \quad (2.88)$$

thus,

$$a(t) = \tilde{B}^{-1/2} \sinh\left(\tilde{B}^{1/2}t\right). \quad (2.89)$$

2.10 Solution of the Friedmann equation with total density

Considering that matter is now a combination of more than two non-interacting fluids, then the next equation 2.90 holds separately for each such fluid f ;

$$\dot{\rho}_f = -3H\left(\rho_f + \frac{P_f}{c^2}\right), \quad (2.90)$$

where in each case

$$\dot{\rho}_f = -3H\left(\rho_f + w_f\rho_f\right), \quad (2.91)$$

from which we obtain

$$\rho_f \propto a^{-3(1+w_f)}. \quad (2.92)$$

Forming a linear combination of such terms (for matter $w_f = 0$; radiation $w_f = 1/3$; dark energy $w_f = -1$),

$$\rho_{\text{tot}} = \rho_{0,r}a^{-4} + \rho_{0,m}a^{-3} + \rho_{0,\Lambda}.$$

Substituting ρ_{tot} into 2.8 gives

$$H^2 = \frac{8\pi G}{3}\left(\rho_{0,r}a^{-4} + \rho_{0,m}a^{-3} + \rho_{0,\Lambda}\right) - \frac{kc^2}{a^2}. \quad (2.93)$$

Multiplying and dividing the right hand side by the critical density at present, $\rho_{c,0} = 3H_0^2/8\pi G$, we arrive at

$$\left(\frac{\dot{a}}{a}\right)^2 = \frac{8\pi G}{3}\rho_{c,0}\left(\Omega_{0,r}a^{-4} + \Omega_{0,m}a^{-3} + \Omega_{0,\Lambda}\right) - \frac{kc^2}{a^2}, \quad (2.94)$$

where $\Omega_{0,r}$, $\Omega_{0,m}$ and $\Omega_{0,\Lambda}$ are the energy density of radiation, dark matter and dark energy, respectively.

$$\implies \dot{a} = \sqrt{\frac{8\pi G}{3}\rho_{c,0}\left(\Omega_{0,r}a^{-2} + \Omega_{0,m}a^{-1} + \Omega_{0,\Lambda}a^2\right) - kc^2}. \quad (2.95)$$

Using $H_0 = 8\pi G\rho_{c,0}/3$ and equation 2.13 we have;

$$\dot{a} = \sqrt{H_0^2\left(\Omega_{0,r}a^{-2} + \Omega_{0,m}a^{-1} + \Omega_{0,\Lambda}a^2\right) + H_0^2(1 - \Omega_0)}, \quad (2.96)$$

where,

$$\Omega_0 = \Omega_{0,r} + \Omega_{0,m} + \Omega_{0,\Lambda}.$$

Taking the integral we have,

$$\int_0^a \left[\left(\Omega_{0,r} a^{-2} + \Omega_{0,m} a^{-1} + \Omega_{0,\Lambda} a^2 \right) + (1 - \Omega_0) \right]^{-1/2} da = H_0 t. \quad (2.97)$$

Assuming the currently accepted and mostly used model, the "Concordance" model, where the universe is said to be nearly flat, we have the following from the Planck data [12]:

$$\begin{aligned} \Omega_{0,m} &= \frac{8\pi G}{3H_0^2} \rho_{0,m} = 0.3089 \pm 0.0062; \\ \Omega_{0,\Lambda} &= \frac{8\pi G}{3H_0^2} \rho_{0,\Lambda} = 0.6911 \pm 0.0062; \\ \Omega_{0,r} &= \frac{8\pi G}{3H_0^2} \rho_{0,r} = 9.06 \times 10^{-5} \pm 0.1233; \end{aligned} \quad (2.98)$$

where we then get the constraint

$$\Omega_0 = \Omega_{0,r} + \Omega_{0,m} + \Omega_{0,\Lambda} \approx 1.$$

In solving the integral 2.97, we use the Trapezoidal rule where the area under a curve is evaluated by dividing the total area into little trapezoids:

$$\int_a^b f(x) dx \approx T_n = \frac{\Delta x}{2} [f(x_0) + 2f(x_1) + 2f(x_2) + \cdots + 2f(x_{n-1}) + f(x_n)]. \quad (2.99)$$

This rule allows us to estimate the area under the curve $f(x)$ to a good approximation, therefore we can also estimate the present age of the Universe in the concordance model:

$$\int_0^1 \left[9.06 \times 10^{-5} a^{-2} + 0.31 a^{-1} + 0.69 a^2 + 9.06 \times 10^{-5} \right]^{-1/2} da = H_0 t. \quad (2.100)$$

$$\implies 0.954828 = H_0 t \implies t = \frac{0.954828}{H_0},$$

$$\therefore t = 13.799 \pm 0.021 \text{ Gyrs.} \quad (2.101)$$

where $H_0 = 0.06928 \text{ Gyr}^{-1}$ is the present value of the Hubble constant [12].

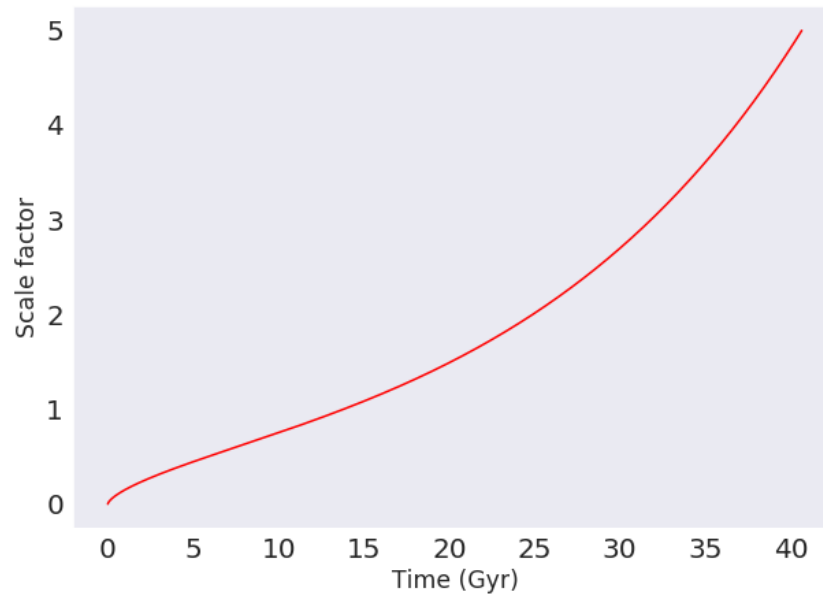


Figure 6: Curve showing the scale factor as function of time for the Concordance model using the constants [2.98](#).

In the next chapter we will introduce a useful technique in dynamical systems, which we will utilize to investigate a generalized system of the Friedmann equations.

3 Dynamical systems in cosmology

The most commonly researched cosmological models have a system of autonomous ordinary differential equations (ODEs) as their governing equations [28]. A dynamical systems method is used since our major purpose is to provide a qualitative description of these models. A short introduction of what dynamical systems are will be given in the next sub-section.

3.1 Dynamical systems

A dynamical system, in general, can be conceived of as any abstract system made up of space (phase space or state space) and a mathematical law that relates the evolution of any point in that space. The state of the system of interest is represented by a set of critical system parameters; and the state space is the collection of all possible values for these parameters. A dynamical system has two main types: continuous and time-discrete.

Continuous dynamical systems are defined by a set of ODEs while time-discrete ones are defined by difference equations or a map [29]. In this context, we are only interested in the type of dynamical systems that are continuous, since we are investigating Friedmann equations, which for an isotropic and homogeneous space result in an ODEs system.

We express the standard form of a dynamical system as

$$\dot{\vec{x}} = \vec{f}(\vec{x}) \quad (3.1)$$

where $\vec{x} = (x_1, x_2, \dots, x_n) \in X$ and X is a subset of \mathbb{R}^n in a representation of a vector of the dynamics of a continuous system, with the dot denoting differentiation with respect to time. The function \vec{f} is sufficiently smooth $\vec{f} : X \rightarrow X$ and a vector field on \mathbb{R}^n

$$\vec{f}(\vec{x}) = (f_1(\vec{x}), \dots, f_n(\vec{x})). \quad (3.2)$$

The concept of a fixed point is crucial when studying a system's local behaviour. We define a fixed point as an equilibrium or constant of a system. A point produced by the autonomous system 3.1 is a fixed point if and only if, for a continuous system, $\vec{f}(\vec{x}_0) = 0$ at a point $\vec{x} = \vec{x}_0$ [30]. We sometimes refer to a fixed point as the critical point, or stationary point. It is possible for a system in \mathbb{R}^n to have no critical point, only one critical point, numerous critical points, or an infinite number of critical points.

One of the methods that can be used to investigate properties of the stability of equilibrium points, is the linear stability theory. To better explain this theory, we consider a mechanical system in one dimension $F(x) = m\ddot{x}$ where F is a force

and suppose there exist a point x_0 where $F(x_0) = 0$. To discover the behaviour of a particle near this point we let $x(t) = x_0 + \delta x(t)$ and suppose that $\delta x(t)$ is very small, then $\ddot{x}(t) = \ddot{\delta x}(t)$ and $F(x) = F(x_0 + \delta x) \approx F(x_0) + F'(x_0)\delta(x) + \dots = F'(x_0)\delta(x) + \dots$, so that our mechanical system equation near the equilibrium point turns out to be $F'(x_0)\delta(x) = m\ddot{\delta x}$ with $F'(x_0)$ being a constant.

Since in this text we aim for working with a system in two dimensions, we consider an autonomous system

$$\begin{aligned}\dot{x} &= f(x, y), \\ \dot{y} &= g(x, y),\end{aligned}\tag{3.3}$$

where f and g are functions of x and y . We suppose the existence of an equilibrium point (x_0, y_0) such that $f(x_0, y_0) = g(x_0, y_0) = 0$. Taking f_x, f_y and g_x, g_y as differentiations of x and y , the Jacobian matrix of 3.3 is

$$J = \begin{pmatrix} f_x & f_y \\ g_x & g_y \end{pmatrix}.\tag{3.4}$$

The eigenvalues of this matrix can then be obtained as

$$\begin{aligned}\lambda_1 &= \frac{1}{2}(f_x + g_y) + \frac{1}{2}\sqrt{(f_x - g_y)^2 + 4f_y g_x}, \\ \lambda_2 &= \frac{1}{2}(f_x + g_y) - \frac{1}{2}\sqrt{(f_x - g_y)^2 + 4f_y g_x},\end{aligned}\tag{3.5}$$

which can be analysed on any equilibrium point (x_0, y_0) . The critical points can be distinguished using the following classification: If the resulting eigenvalues have negative real parts, then that point can be regarded as stable. If at least one of the eigenvalues has a real part that is positive, then the critical point involved would be unstable and thus correlate with a saddle point which attracts and repels trajectories in some directions. Finally, the eigenvalues could all have positive real parts, in which the critical point would be regarded as unstable and the trajectories repel [29].

In table 1 we present all the possible cases for an autonomous system in two dimensions like equations 3.3. The exact same technique described above can be used when analysing arbitrary dynamical systems, as a result we will utilize it in the context of cosmology in order to carry out our analysis.

Table 1: Combinations of eigenvalues λ_1 and λ_2 showing the stability or instability properties of an equilibrium point (x_0, y_0) .

Eigenvalues	Explanation
$\lambda_1 > 0$ and $\lambda_2 > 0$	the critical point is not stable and the trajectories are repelled from the point (x_0, y_0) . This point may be referred to as the past attractor.
$\lambda_1 < 0, \lambda_2 > 0$	the equilibrium point is a saddle point. While some paths will be repulsed, the others will be attracted.
$\lambda_1 < 0, \lambda_2 < 0$	the critical point is stable and the trajectories that start close by this point will advance toward that point (X_0, y_0) .
$\lambda_1 = 0, \lambda_2 > 0$	the equilibrium point is not stable. The positive eigenvalue guarantees that there's at least one direction that is unstable.
$\lambda_1 = 0, \lambda_2 < 0$	the stability of this combination cannot be determined using the linear stability theory as it breaks down, thus other methods are needed.
$\lambda_{1,2} = \pm i\beta$	the trajectories are oscillatory and we refer to the point as the centre.
$\lambda_{1,2} = \alpha \pm i\beta$	the critical point is stable and spiral if $\alpha < 0$ and $\beta \neq 0$. But if $\alpha > 0$ then the point is unstable.

3.2 Defining parameters

With a spatially flat universe $k = 0$ filled with radiation, matter and dark energy assumed, we start first by giving the Friedmann equation;

$$\begin{aligned}
 H^2 &= \frac{8\pi G}{3} \left(\rho_r + \rho_m + \rho_{\text{DE}} \right) \\
 &= \frac{8\pi G}{3} \rho_r + \frac{8\pi G}{3} \rho_m + \frac{8\pi G}{3} \rho_{\text{DE}} \\
 1 &= \frac{8\pi G}{3H^2} \rho_r + \frac{8\pi G}{3H^2} \rho_m + \frac{8\pi G}{3H^2} \rho_{\text{DE}} \\
 &= \Omega_r + \Omega_m + \Omega_{\text{DE}}
 \end{aligned} \tag{3.6}$$

where

$$\Omega_r \equiv \frac{8\pi G}{3H^2} \rho_r \quad ; \quad \Omega_m \equiv \frac{8\pi G}{3H^2} \rho_m \quad ; \quad \Omega_{\text{DE}} \equiv \frac{8\pi G}{3H^2} \rho_{\text{DE}} \tag{3.7}$$

are the fractional energy densities of radiation, matter and dark energy; respectively. Furthermore, because we expect positive energy densities, we have the conditions $0 \leq \Omega_r \leq 1$ and $0 \leq \Omega_m \leq 1$. As a result, the condition $\Omega_{\text{DE}} \leq 1$ is also required in order to satisfy 3.6.

3.3 Cosmological dynamical systems set up

Taking a dimensionless value of the speed of light $c = 1$, we may rewrite (2.20) and give the general equation for perfect fluid as

$$\dot{\rho} + 3H(1 + w)\rho = 0 \tag{3.8}$$

where $H = \dot{a}/a$. Knowing that for radiation and matter, $w_r = 1/3$ and $w_m = 0$, we can write,

$$\dot{\rho}_r + 4H\rho_r = 0 \quad ; \quad \dot{\rho}_m + 3H\rho_m = Q \quad ; \quad \dot{\rho}_{\text{DE}} + 3H(1 + w_{\text{DE}})\rho_{\text{DE}} = -Q, \tag{3.9}$$

where we have taken into account the Interaction (denoted by Q) between dark matter and dark energy. The positive sign of Q in (3.9) indicates transition of contents of energy from dark energy to dark matter (baryonic matter, which makes 15.7% of $\Omega_{0,m}$ is excluded in this consideration); and for a negative Q , the process is reversed [31]. This is also to ensure that total matter is conserved in the universe. The sum of equations 3.9 gives the total energy conservation in the universe as $\dot{\rho} + 3H(\rho_{\text{tot}} + P_{\text{eff}}) = 0$, where the total equation of state can be written as

$$w_{\text{eff}} = \frac{P_{\text{eff}}}{\rho_{\text{tot}}} = -1 - \frac{2\dot{H}}{3H^2}. \tag{3.10}$$

where ρ_{tot} and P_{eff} are the total energy density and effective pressure, respectively. Defining the energy density for dark energy [32,33] as

$$\rho_{\text{DE}} = \alpha H + \beta H^2 \quad (3.11)$$

leads to

$$\rho_{\text{DE}} \dot{=} \alpha \dot{H} + 2\beta H \dot{H}, \quad (3.12)$$

where α and β are constants with dimension $(\text{mass})^3$ and $(\text{mass})^2$ respectively. The model defined by 3.11 is considered since it alleviates the fine-tuning problem [31]. Substituting in the equations 3.9 leads to;

$$\alpha \dot{H} + 2\beta H \dot{H} + 3H(1 + w_{\text{DE}})\rho_{\text{DE}} = -Q \quad (3.13)$$

$$\implies 3H(1 + w_{\text{DE}})\rho_{\text{DE}} + Q = -\dot{H}(\alpha + 2\beta H) \quad (3.14)$$

$$\implies \frac{H(1 + w_{\text{DE}})\rho_{\text{DE}} + Q}{H\rho_{\text{DE}}} = -\frac{\dot{H}(\alpha + 2\beta H)}{H^2(\alpha + \beta H)} \quad (3.15)$$

where on the last equation we have divided by $H\rho_{\text{DE}} = \alpha H^2 + \beta H^3$ on both sides. By equations 3.6 we have that

$$\dot{\rho}_{\text{r}} + \dot{\rho}_{\text{m}} + \dot{\rho}_{\text{DE}} = \frac{3\dot{H}H}{4\pi G}, \quad (3.16)$$

hence 3.9 leads to,

$$\begin{aligned} -4H\rho_{\text{r}} - 3H\rho_{\text{m}} + Q - 3H(1 + w_{\text{DE}})\rho_{\text{DE}} - Q &= \frac{3\dot{H}H}{4\pi G} \\ -4\rho_{\text{r}} - 3\rho_{\text{m}} - 3(1 + w_{\text{DE}})\rho_{\text{DE}} &= \frac{3\dot{H}}{4\pi G} \\ -2\frac{8\pi G}{3H^2}\rho_{\text{r}} - \frac{3}{2}\frac{8\pi G}{3H^2}\rho_{\text{m}} - \frac{3}{2}\frac{8\pi G}{3H^2}\rho_{\text{DE}}(1 + w_{\text{DE}}) &= \frac{\dot{H}}{H^2} \\ -2\Omega_{\text{r}} - \frac{3}{2}\Omega_{\text{m}} - \frac{3}{2}\Omega_{\text{DE}}(1 + w_{\text{DE}}) &= \frac{\dot{H}}{H^2} \\ -\frac{1}{2}\left[4\Omega_{\text{r}} + 3\Omega_{\text{m}} + 3\Omega_{\text{DE}}(1 + w_{\text{DE}})\right] &= \frac{\dot{H}}{H^2}. \end{aligned} \quad (3.17)$$

Now, first working out the deceleration parameter, q , we have that since $H = \dot{a}/a$;

$$\begin{aligned} \dot{H} &= \frac{\ddot{a}}{a} - \frac{\dot{a}^2}{a^2} = \frac{\ddot{a}}{a} - H^2, \\ -\frac{\dot{H}}{H^2} &= -\frac{\ddot{a}}{aH^2} + 1 = q + 1, \end{aligned} \quad (3.18)$$

where $q = -\ddot{a}/aH^2$, thus the deceleration parameter is;

$$\begin{aligned} q &= -\left(1 + \frac{\dot{H}}{H^2}\right), \\ q &= -1 + \frac{1}{2} \left[4\Omega_r + 3\Omega_m + 3\Omega_{\text{DE}}(1 + w_{\text{DE}})\right]. \end{aligned} \quad (3.19)$$

Solving the equation of state (EoS) parameter for dark energy, w_{DE} , by equation 3.15 we have;

$$w_{\text{DE}} = -\frac{\dot{H}(\alpha + 2\beta H)}{H^2(\alpha + \beta H)} - \frac{Q}{H\rho_{\text{DE}}} - 1. \quad (3.20)$$

After substituting eq. (3.20) into (3.17) and solving for w_d we found that;

$$w_{\text{DE}} = \frac{2(\alpha + \beta H)}{2(\alpha + \beta H) - 3\Omega_{\text{DE}}(\alpha + 2\beta H)} \left[\frac{(4\Omega_r + 3\Omega_m)(\alpha + 2\beta H)}{2(\alpha + \beta H)} + \frac{3(\alpha + 2\beta H)\Omega_{\text{DE}}}{2(\alpha + \beta H)} - \frac{Q}{H\rho_{\text{DE}}} - 1 \right].$$

Noting that $\rho_{\text{DE}} = (3H^2/8\pi G)\Omega_{\text{DE}}$ and defining $\Omega_q \equiv (8\pi G/3H^2)Q$, we obtain:

$$w_{\text{DE}} = \frac{\alpha[2\Omega_q - H\Omega_{\text{DE}}(3(\Omega_{\text{DE}} + \Omega_m - 2) + 4\Omega_r)] + 2\beta H[\Omega_q - H\Omega_{\text{DE}}(3(\Omega_{\text{DE}} + \Omega_m - 1) + 4\Omega_r)]}{3H\Omega_{\text{DE}}[\alpha(\Omega_{\text{DE}} - 2) + 2\beta H(\Omega_{\text{DE}} - 1)]},$$

We define a new system by first defining new dimensionless variables as follows:

$$x^2 = \Omega_m; \quad y^2 = \frac{8\pi G\alpha}{3H}; \quad m^2 = \frac{8\pi G\beta}{3}; \quad y^2 + m^2 = \Omega_\Lambda, \quad (3.21)$$

with the radiation parameter consequently given as $\Omega_r = 1 - m^2 - x^2 - y^2$. Using (3.21), and doing some algebra, we can finally write w_Λ , w_{eff} and q as:

$$w_\Lambda = \frac{2m^4 + m^2(2x^2 + 3y^2 - 2) + y^2(x^2 + y^2 + 2) + 2f(x, y)}{3(m^2 + y^2)(2m^2 + y^2 - 2)}, \quad (3.22)$$

$$w_{\text{eff}} = \frac{2(m^2 + x^2 - 1) + 5y^2 + 2f(x, y)}{3(2m^2 + y^2 - 2)}, \quad (3.23)$$

and

$$q = \frac{2m^2 + x^2 + 3y^2 - 2 + f(x, y)}{2m^2 + y^2 - 2}, \quad (3.24)$$

where $f(x, y) = \Omega_q/H$. Letting $N = \ln(a)$, then the dynamical equations take the form

$$x' = \frac{1}{2x} \frac{dx^2}{dN}; \quad y' = \frac{1}{2y} \frac{dy^2}{dN}, \quad (3.25)$$

which implies,

$$\begin{aligned} x' &= \frac{x^2(2m^2 + 2x^2 + 5y^2 - 2) + f(x, y)(2m^2 + 2x^2 + y^2 - 2)}{2x(2m^2 + y^2 - 2)}, \\ y' &= \frac{y[(4m^2 + x^2 + 4y^2 - 4) + f(x, y)]}{4m^2 + 2y^2 - 4}. \end{aligned} \quad (3.26)$$

The parameter y satisfies the condition $0 < y < 1$ (so that 3.26 are continuous). The dimensionless variable m^2 is significant for the early evolution of the universe, otherwise it is a negligible value. It has been shown by [32] that m^2 could have a fraction energy density of approximately 10 percent in the early universe hence in this text we will refer to m^2 as the early dark energy (EDE) term. That is to say, the parameter m always satisfies the constraint $0 < m^2 \leq 0.1$. We also name the y^2 part of the Ω_{DE} as late dark energy (LDE).

In the next chapter we look at different terms of interaction Q in order to investigate the most likely form of the interaction between dark matter and dark energy; and present the results.

4 The evolution of interacting DE models

In cosmology, theories in which DM and DE interact play a crucial role, having been inspired to tackle the cosmological constant problem and thereafter the coincidence problem. Due to their capacity to handle the well-known conflicts between high and low redshift estimates of the Hubble constant H_0 and the value of the amplitude of the power spectrum σ_8 , interacting dark energy theories have lately seen a renewed wave of attention [34, 35]. Because they provide for an energy exchange mechanism between the dark sector components, such interacting situations are exceedingly generic. As a consequence of the unknown nature and dynamics of DE and DM, it makes it strenuous to narrate on these components from first principles with regard to established theories, thus leaving more room to construct models.

In this chapter, we therefore take a deeper look at the evolution equations by investigating some of the possible interaction models [15, 31, 36] between dark matter and dark energy.

4.1 Possible couplings of DM and DE

(A) No interaction: $Q = 0$

When there is no interaction between dark matter and dark energy, $f(x, y) = 0$, the dynamical equations (3.26) are said to be smooth (or continuous) and in this case there are three acceptable points:

- $P_1: (x, y) = (0, 0)$. This point describes the early stages of the universe, meaning that matter and the late dark energy did not contribute to the content of the energy of the universe. Both the eigenvalues of the linearization matrix $\lambda_1 = 1/2$ and $\lambda_2 = 1$ are positive, which shows the instability of this phase. Using eq. (3.23) and (3.24) we see that $w_{\text{eff}} = 1/3$, and $q = 1$ which represents the deceleration expansion of this epoch.
- $P_2: (x, y) = (\sqrt{1 - m^2}, 0)$. From this point we can deduce that it illustrates the dark matter epoch of the universe, which is basically the matter dominated phase. From the linearization matrix, we obtain the eigenvalues $\lambda_1 = -1$ and $\lambda_2 = 3/4$, implying an unstable phase. We also find that the effective EoS and deceleration parameter are, $w_{\text{eff}} = 0$ and $q = 1/2$.
- $P_3: (x, y) = (0, \sqrt{1 - m^2})$. Since we refer to y^2 as the late dark energy and remembering that m^2 takes very small values at late times, we can say that the point P_3 illustrates the LDE dominated universe. The eigenvalues found were both negative, $\lambda_1 = -3/2$ and $\lambda_2 = -4$ which suggest that this epoch

is stable. We also found that $w_{\text{eff}} = -1$ and $q = -1$. The deceleration being $q < 0$ implies that this phase is undergoing acceleration.

In figure (7), we show the phase plane for the case where $Q = 0$, that is, when there is no interaction. As can easily be seen on this figure, all the field lines end at the $(x, y) = (0, 1)$ point; which is consistent with the dark energy dominated universe. We can label the paths of figure (7) as true cosmological paths as they begin at the unstable radiation phase $(x = 0, y = 0)$, passing through unstable matter phase $(x \approx 1, y = 0)$ and ending at the stable dark energy dominated point $(x = 0, y = 1)$.

Figure 7a shows the phase space evolution for the case $Q = 0$, where all three fixed points are well represented. In 7b the cosmic evolution of the energy density Ω_i is presented. The initial conditions are chosen at present as $\Omega_{0,r} = 9.06 \times 10^{-5}$, $\Omega_{0,m} = 0.31$ and $\Omega_{0,\Lambda} = 0.69$. Figure 7c shows the evolution of the equation of state together with the deceleration parameter.

(B) Linear interaction: $Q = 3b^2 H \rho_{\text{tot}}$

Since $f(x, y) = \Omega_q/H$ and $\Omega_q = (8\pi G/3H^2)Q$, we have

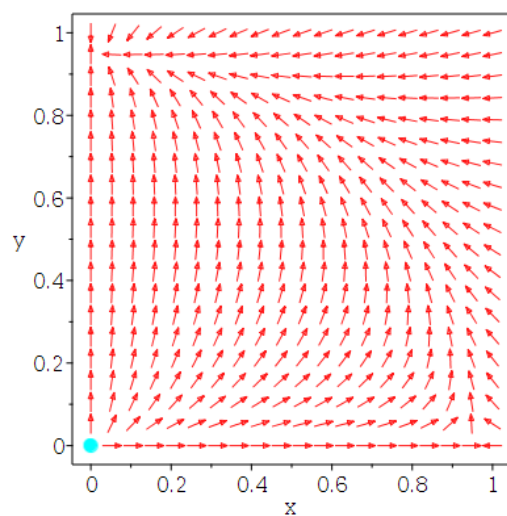
$$f(x, y) = \frac{8\pi G}{3H^3} Q = \frac{8\pi G}{3H^2} (\rho_r + \rho_m + \rho_\Lambda) 3b^2 = 3b^2.$$

We then find that the dynamical equations (3.26) now take the form

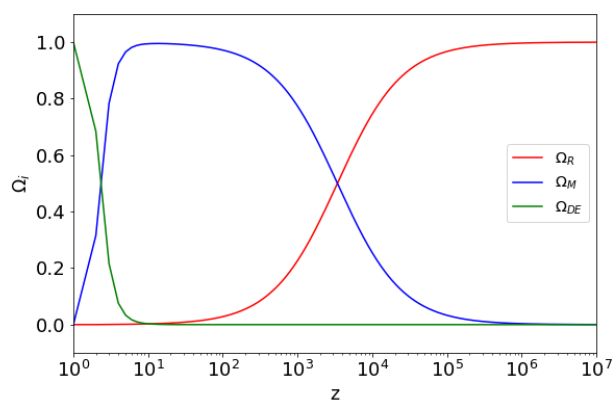
$$\begin{aligned} x' &= \frac{x^2(2m^2 + 2x^2 + 5y^2 - 2) + 3b^2(2m^2 + 2x^2 + y^2 - 2)}{2x(2m^2 + y^2 - 2)}, \\ y' &= \frac{y[(4m^2 + x^2 + 4y^2 - 4) + 3b^2]}{4m^2 + 2y^2 - 4}. \end{aligned} \quad (4.1)$$

Investigating (4.1) we obtain the following points:

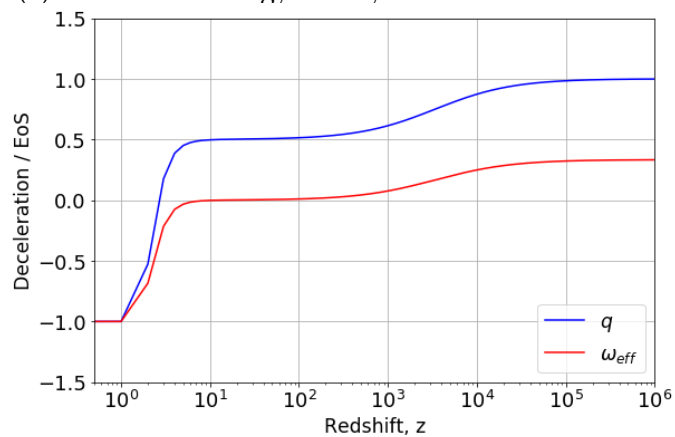
- $P_1: (x, y) = (\sqrt{1 - m^2}, 0)$. The following eigenvalues correspond to this point: $\lambda_1 = -3b^2 - 1 \approx -1$ and $\lambda_2 = -3b^2/4 + 3/4 \approx 3/4$, from which we conclude that this point is unstable. The effective EoS and deceleration parameters were calculated as, $w_{\text{eff}} = -b^2/(1 - m^2) \sim 0$ and $q = 1/2(1 - 3b^2/(1 - m^2)) \sim 1/2$ (since both m^2 and b are small parameters), respectively. This point is consistent with the matter dominated epoch of the universe.
- $P_2: (x, y) = (b, \sqrt{1 - b^2 - m^2})$. With the eigenvalues $\lambda_1 = -4$ and $\lambda_2 = 3(b^2 - 1)/(b^2 - 1) \sim -3$, since at late times the parameter m^2 is small, we



(a) Phase space evolution



(b) Evolution of energy density as a function of redshift



(c) Deceleration and EoS parameter vs. redshift.

Figure 7: Evolution plots for the first interaction case.

conclude that this equilibrium point is stable. This point describes the late dark energy scaling solution. We also discover that $q = -1$ and $w_{\text{DE}} = 1/(b^2 - 1) < -1$.

Performing the same analysis as in the first model, on the phase space of figure 8a, we cannot make similar conclusions with the model (B), since we do not have a unique starting point for the paths shown. Therefore according to this linear interaction solution, the model suffers from the absence of radiation dominated era at the early times, which is due to the discontinuity of the system 4.1 near the point (0,0).

Figure 8a shows the evolution of phase space for the linear interaction (B) where we have chosen $b = 0.2$. Initial conditions are chosen as $\Omega_{0,r} = 1 \times 10^{-5}$, $\Omega_{0,m} = 0.04$ and $\Omega_{0,\Lambda} = 0.96$. This model breaks down at the radiation dominated fixed point. Due to lack of a fixed point, 8b only shows the cosmic evolution for matter and dark energy. The evolution of EoS and the deceleration parameters are shown in 8c.

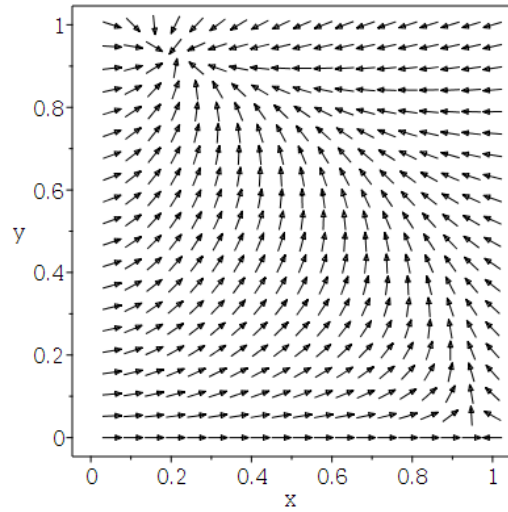
(C) Non-linear interaction: $Q = 3b^2 H \rho_{\text{DE}} \rho_{\text{m}} / \rho_{\text{tot}}$

With this non-linear interaction case, we find, from equations 3.7 and 3.21 that; $f(x, y) = 3b^2 x^2 (y^2 + m^2)$, which 3.26 then leads to a new form of dynamical equations:

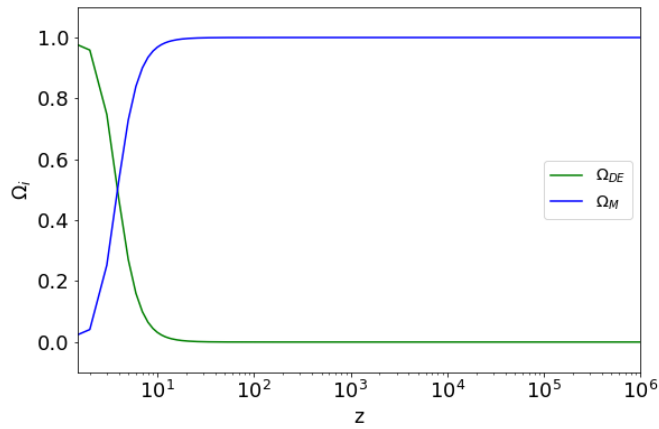
$$\begin{aligned} x' &= \frac{x[y^2(b^2(9m^2 + 6x^2 - 6) + 5) + 2(3(bm)^2 + 1)(m^2 + x^2 - 1) + 3(by^2)^2]}{4m^2 + 2y^2 - 4}, \\ y' &= \frac{y[m^2(3(bx)^2 + 4) + 3(bxy)^2 + x^2 + 4(y^2 - 1)]}{4m^2 + 2y^2 - 4}. \end{aligned} \quad (4.2)$$

In solving 4.2, three physically acceptable critical points are obtained:

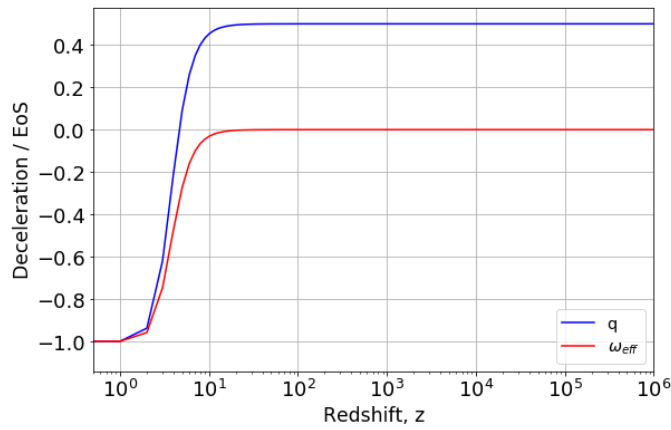
- $P_1 : (x, y) = (0, 0)$. The calculated eigenvalues $\lambda_1 = 1$ and $\lambda_2 = 1/2$ indicates the instability of this point. Using equations 3.23 and 3.24, we identify EoS and deceleration parameter as $w_{\text{eff}} = 1/3$ and $q = 1$, respectively. We can then say that this is a radiation dominated era.
- $P_2 : (x, y) = (\sqrt{1 - m^2}, 0)$. According to the pair of eigenvalues, $\lambda_1 = 3/4$ and $\lambda_2 = -1$, this is an unstable equilibrium point. We also find that $w_{\text{eff}} = -(bm)^2 > -1/3$ and $q = 1/2(1 - 3(bm)^2) > 0$ implies deceleration of matter. This point correlates with the dark matter dominated epoch.
- $P_3 : (x, y) \approx (0, \sqrt{1 - m^2})$. A stable fixed point is implied by the corresponding eigenvalues of this point: $\lambda_1 = -4$ and $\lambda_2 \sim -3/2$. Recalling



(a) Phase space evolution



(b) Evolution of energy density as a function of redshift



(c) Deceleration parameter and EoS versus redshift.

Figure 8: Evolution plots for the interaction case **B**.

that the parameter m^2 is very small at late times, we have P_3 correlating to the dark energy dominated epoch. The following values are also obtained; $w_{\text{eff}} = w_\Lambda = -1$ and $q = -1$.

(D) Non-linear interaction: $Q = 3b^2 H \rho_m^2 / \rho_{\text{tot}}$

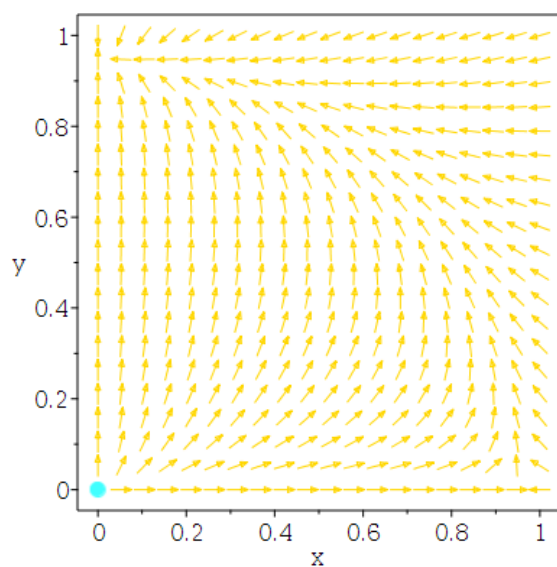
With this particular interaction, equation 3.26, and noting (3.7) and 3.21, leads us to a set of new dynamical equations, namely

$$\begin{aligned} x' &= \frac{1}{2}x \left[\frac{2(3(bx^2)^2 - 4m^2 + x^2 + 4)}{2m^2 + y^2 - 2} + 3(bx)^2 + 5 \right], \\ y' &= \frac{y[3(bx^2)^2 + 4m^2 + x^2 + 4(y^2 - 1)]}{2(2m^2 + y^2 - 2)}. \end{aligned} \quad (4.3)$$

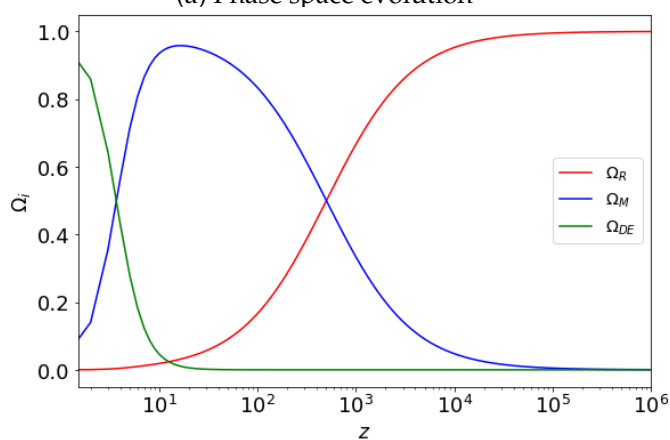
We now analyse (4.3) at these three physically acceptable critical points;

- $P_1 : (x, y) = (0, 0)$. Corresponding to this critical point are the eigenvalues $\lambda_1 = 1$ and $\lambda_2 = 1/2$, which suggest an unstable point. By using 3.23 and 3.24 we then get $w_{\text{eff}} = 1/3$ and $q = 1$. Radiation scaling phase is demonstrated by this critical point.
- $P_2: (x, y) = (\sqrt{1 - m^2}, 0)$. With this critical point we find that $w_{\text{eff}} = -b^2(1 - m^2)$ and $q = 1/2(1 - 3b^2(1 - m^2))$. In determining a matter dominated phase, we know that $w_{\text{eff}} > -1/3$ and $q > 0$ which leads to the constrain $b < 1/\sqrt{3(1 - m^2)}$. This is an unstable (due to $\lambda_1 = -1$ and $\lambda_2 = 3/4$) matter dominated epoch.
- $P_3: (x, y) = (0, \sqrt{1 - m^2})$. The eigenvalues $\lambda_1 = -3/2$ and $\lambda_2 = -4$ suggest this point is stable. As usual, using equation 3.23 and 3.24, the parameters $w_{\text{eff}} = -1$ and $q = -1$ are obtained, which is consistent with the standard Λ CDM solutions. This is a late dark energy phase shown by this point.

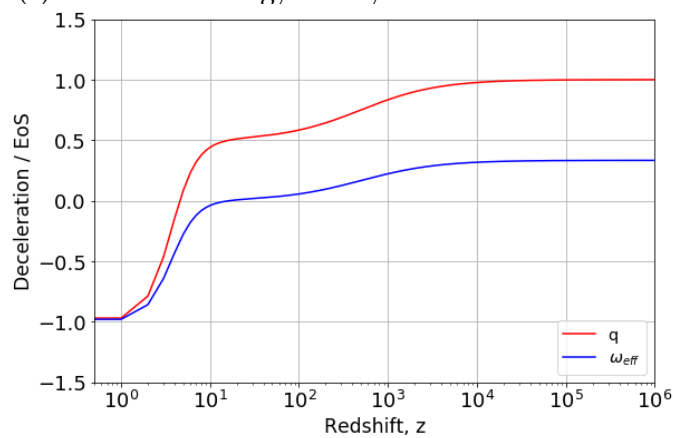
With interactions (C) and (D) having similar sets of critical points, and displaying exactly the same paths; in figure 9a we represent their phase space evolution, where $b = 0.2$ is chosen and initial conditions were chosen as $\Omega_{0,r} = 0.0, \Omega_{0,m} = 0.02$ and $\Omega_{0,\Lambda} = 0.98$. In 9b, the cosmic evolution Ω_i is presented. Figure 9c represents the evolution of the deceleration and EoS parameters.



(a) Phase space evolution



(b) Evolution of energy density as a function of redshift



(c) Deceleration and EoS parameter vs. redshift.

Figure 9: Evolution plots for the interaction case C and D.

(E) Non-linear interaction: $Q = 3b^2 H \rho_{\text{DE}}^2 / \rho_{\text{tot}}$

A new form of equation 3.26 is obtained as,

$$\begin{aligned} x' &= \frac{x^2(2m^2 + 2x^2 + 5y^2 - 2) + 3b^2(x^2 + y^2 - 1)^2(2m^2 + 2x^2 + y^2 - 2)}{2x(2m^2 + y^2 - 2)}, \\ y' &= \frac{y[3b^2(x^2 + y^2 - 1)^2 + 4m^2 + x^2 + 4(y^2 - 1)]}{4m^2 + 2y^2 - 4}. \end{aligned} \quad (4.4)$$

Investigating 4.4 at the three different physically acceptable critical points, we have the following,

- $P_1: (x, y) = (\sqrt{1 - m^2}, 0)$. From $\lambda_1 = 3/4$ and $\lambda_2 = -1$, we read that this equilibrium point is unstable. We also get that the deceleration parameter is $q = 1/2 + 3(bm^2)^2 / (2(m^2 - 1))$; and effective EoS as $w_{\text{eff}} = -(bm^2)^2 \sim 0$. By this point, EDE phase is shown.
- $P_2: (x, y) \approx (bm^2, \sqrt{1 - m^2})$. Because of the pair of eigenvalues $\lambda_1 = -3/2$ and $\lambda_2 = -4$, this a stable fixed point. For this point, we also find that $w_{\text{eff}} = -3/3 = -1$ and $q = -1$. As the constant m^2 is small at late times, this critical point demonstrates a dark energy dominated epoch of the universe.
- P_3 : Due to this point being very messy to include in this text, it is omitted, but upon checking, it also displayed trends of the dark energy epoch.

(F) Non-linear interaction: $Q = 3b^2 H \rho_{\text{DE}}^3 / \rho_{\text{tot}}^2$

For the function f we get $f(x, y) = 3b^2(m^2 + y^2)^3$, thus from 3.26 the following system of equations is obtained for this interaction:

$$\begin{aligned} x' &= \frac{x^2[2(m^2 + x^2 - 1) + 5y^2] + 3b^2(m^2 + y^2)^3[2(m^2 + x^2 - 1) + y^2]}{2x(2m^2 + y^2 - 2)}, \\ y' &= \frac{y[3(bm^3)^2 + (3bm^2y)^2 + m^2(9b^2y^4 + 4) + 3b^2y^6 + x^2 + 4(y^2 - 1)]}{4m^2 + 2y^2 - 4}. \end{aligned} \quad (4.5)$$

Analysing 4.5 at various acceptable points we have the following:

- $P_1 : (x, y) \approx (0, 0)$. The corresponding eigenvalues are $\lambda_1 = 0$ and $\lambda_2 = 1$ which implies that this equilibrium point is not stable. A radiation dominated phase by this point is implied, from which we also get $w_{\text{eff}} = 1/3$ and $q = 1$.

- $P_2: (x, y) = (\sqrt{1 - m^2}, 0)$. Corresponding to this fixed point are the eigenvalues $\lambda_1 = 3/4$ and $\lambda_2 = -1$ which confirm the instability of this point. With this point we notice dark matter phase where $w_{\text{eff}} = -b^2 m^6 \sim 0$ and $q = 1/2 + 3b^2 m^6 / (2(m^2 - 1)) > 0$.

(G) Interaction: $Q = 3b^2 H \rho_m$

With this choice of interaction, since $f(x, y) = \Omega_q / H$ and $\Omega_q = (8\pi G / 3H^2) Q$, we have the following:

$$f(x, y) = \frac{8\pi G}{3H^3} Q = \frac{8\pi G}{3H^3} (3b^2 H \rho_m) = \frac{9}{8} b^2 \left(\frac{8\pi G}{3H^2} \rho_m \right) = 3b^2 x^2. \quad (4.6)$$

We then find that the dynamical equations (3.26) now take the form

$$\begin{aligned} x' &= \frac{x(2m^2 + 2x^2 + 5y^2 - 2) + 3b^2 x(2m^2 + 2x^2 + y^2 - 2)}{2(2m^2 + y^2 - 2)}, \\ y' &= \frac{y[(4m^2 + x^2 + 4y^2 - 4) + 3b^2 x^2]}{2(2m^2 + y^2 - 2)}. \end{aligned} \quad (4.7)$$

We now analyse 4.7 at these three physically acceptable critical points;

- $P_1 : (x, y) = (0, 0)$. Using equations (3.23) and (3.24) we see that $w_{\text{eff}} = 1/3$ and $q = 1$. This is a radiation dominated epoch. Furthermore, the eigenvalues $\lambda_1 = 1$ and $\lambda_2 \sim 1/2$ are both positive, thus confirming the instability of the radiation era.
- $P_2: (x, y) = (\sqrt{-m^2 + 1}, 0)$. From (3.23) and (3.24) we read that $w_{\text{eff}} = -(3/8)b^2 \sim 0$ and $q = 1/2 - (9/16)b^2 \sim 1/2$ since b is very small. Since the eigenvalues $\lambda_1 = -1$ and $\lambda_2 \sim 3/4$ are positive and negative, the instability of the matter dominated era is confirmed.
- $P_3: (x, y) = (0, \sqrt{1 - m^2})$. The calculated eigenvalues were $\lambda_1 = -3/2$ and $\lambda_2 = -4$, implying that the epoch of DE is stable with the EoS being $w_{\text{eff}} = -1$. The deceleration parameter was also found as $q = -1$.

(H) Interaction: $Q = 3b^2 H \rho_{\text{DE}}$

For this type of interaction Q , we have the function $f(x, y) = \Omega_q / H$ as follows:

$$f(x, y) = \frac{8\pi G}{H^3} Q = 3b^2 \left(\frac{8\pi G}{3H^2} \rho_{\text{DE}} \right) = 3b^2 \Omega_\Lambda = 3b^2 (y^2 + m^2).$$

The new set of dynamical equations is then;

$$\begin{aligned} x' &= \frac{x^2(2m^2 + 2x^2 + 5y^2 - 2) + 3b^2(y^2 + m^2)(2m^2 + 2x^2 + y^2 - 2)}{2x(2m^2 + y^2 - 2)}, \\ y' &= \frac{y[(4m^2 + x^2 + 4y^2 - 4) + 3b^2(y^2 + m^2)]}{4m^2 + 2y^2 - 4}. \end{aligned} \quad (4.8)$$

Analysing this system, the following fixed points are obtained:

- $P_1: (x, y) = (\sqrt{-m^2 + 1}, 0)$. The corresponding eigenvalues of this fixed point; $\lambda_1 = 3/4$ and $\lambda_2 = -1$, implies an unstable matter-dominated universe. The EoS was approximated as $w_{\text{eff}} \approx 0$ since the m^2 is small. The deceleration for this point was $q = 1/2$.
- $P_2: (x, y) = (\frac{1}{b^2+1}, \frac{1}{b^2+1} - m^2)$. Eigenvalues $\lambda_1 = -5 + \sqrt{41}/2$ and $\lambda_2 = -5 - \sqrt{41}/2$. This is a stable late dark energy epoch. Calculation of the EoS gives $w_{\text{eff}} = -5/3$ while deceleration gives $q < -17/10$.

(I) Interaction: $Q = \eta\rho_m$

We now analyse another type of interaction which is different from the other interaction models that we have already studied in the previous subsections. Here, we introduce the transfer rate $\eta = \gamma H_0$ where γ is a dimensionless constant. Therefore, for the function f , the following equation is obtained;

$$f(x, y) = \frac{8\pi G}{H^3} Q = \frac{\eta}{H} \left(\frac{8\pi G}{3H^2} \rho_m \right) = \frac{\eta}{H} \Omega_m = \frac{\eta}{H} x^2. \quad (4.9)$$

To keep the dimensionality the same, we introduce a new dimensionless parameter v given as;

$$v = \frac{H_0}{H + H_0} \quad (4.10)$$

where $0 \leq v < 1$. We now obtain a new function f given as

$$f(x, y) = \frac{\eta}{H} x^2 = \gamma \frac{H_0}{H} x^2 = \gamma \left(\frac{v}{1-v} \right) x^2. \quad (4.11)$$

Thus, the set of new dynamical equations is:

$$\begin{aligned} x' &= \frac{(1-v)x^2(2m^2 + 2x^2 + 5y^2 - 2) + \gamma v x^2(2m^2 + 2x^2 + y^2 - 2)}{2(1-v)x(2m^2 + y^2 - 2)}, \\ y' &= \frac{y[(1-v)(4m^2 + x^2 + 4y^2 - 4) + \gamma v x^2]}{2(1-v)(2m^2 + y^2 - 2)}. \end{aligned} \quad (4.12)$$

From the above system 4.12 we arrive at a set of three acceptable critical points;

- $P_1 : (x, y) = (0, 0)$. The corresponding eigenvalues $\lambda_1 = 1$ and $\lambda_2 = -(\gamma v - v + 1)/(2(-1 + v)) \sim 1/2$, suggest that we have an unstable fixed point. The EoS is $w_{\text{eff}} = -(-2 + 2v)/(6(1 - v)) = 1/3$ while deceleration is $q = 1$.
- $P_2: (x, y) = (\sqrt{1 - m^2}, 0)$. The eigenvalues $\lambda_1 = (\gamma v - v + 1)/(-1 + v) \sim -1$ and $\lambda_2 = \gamma v/(4(-1 + v)) + 3/4 > 0$ show an unstable matter dominated epoch. The EoS and deceleration are $w_{\text{eff}} = -\gamma v(3(1 - v)) \sim 0$ and $q = -\gamma v + 1/2 \sim 1/2$, respectively.
- $P_3: (x, y) = (0, \sqrt{1 - m^2})$. Eigenvalues were found as, $\lambda_1 = -4$ and $\lambda_2 \sim -3/2$ which show that this point is stable. The equation of state is $w_{\text{eff}} = -(3 + 2v)/(3(1 - v)) \leq -1$, and for the the deceleration, $q = -1$ was calculated for this fixed point.

(J) Interaction: $Q = 3b^2 H(\rho_{\text{DE}} + \rho_m)$

For this late interaction term, we obtain the following

$$f(x, y) = 3b^2(y^2 + x^2 + m^2), \quad (4.13)$$

and thus a set of dynamical equations of the form

$$\begin{aligned} x' &= \frac{x^2(2m^2 + 2x^2 + 5y^2 - 2) + 3b^2(y^2 + x^2 + m^2)(2m^2 + 2x^2 + y^2 - 2)}{2x(2m^2 + y^2 - 2)}, \\ y' &= \frac{y[(4m^2 + x^2 + 4y^2 - 4) + 3b^2(y^2 + x^2 + m^2)]}{4m^2 + 2y^2 - 4}. \end{aligned} \quad (4.14)$$

Calculating and analysing the critical points from the set above, we draw the following conclusions:

- $P_1: (x, y) = (\sqrt{1 - m^2}, 0)$. The eigenvalues for this epoch $\lambda_1 = 3/4$ and $\lambda_2 = -1$ show that this point is unstable, with the EoS and deceleration parameter calculated as $w_{\text{eff}} = 0$ and $q = 1/2$, respectively.
- $P_2: (x, y) = (b, \sqrt{1 - b^2 - m^2})$. With the corresponding eigenvalues being $\lambda_1 = -4$ and $\lambda_2 \sim -3$, we confirm the stability of this point. The EoS and deceleration were $w_{\text{eff}} = -1$ and $q = -1$, respectively.

4.2 Trends in the studied interaction models

In this section we compare and explore the trends in our interaction models. As shown on the first interaction, model (A), the cosmological paths which we expected, we were able to observe on the phase space plot. The fractional energy

density plot showed dominance of the radiation era in the early times of the universe and then it became less dominant when the next epoch of matter took over. The last epoch to dominate is the dark energy era, which is currently dominating our universe. We demonstrate this behaviour for the first three of our models on figure 10. Similar behaviours with the interaction models **C**, **D**, **F**, **G**, and **I** were also observed. However, we also analysed models, such as models **B**, **E**, **H** and **J**,

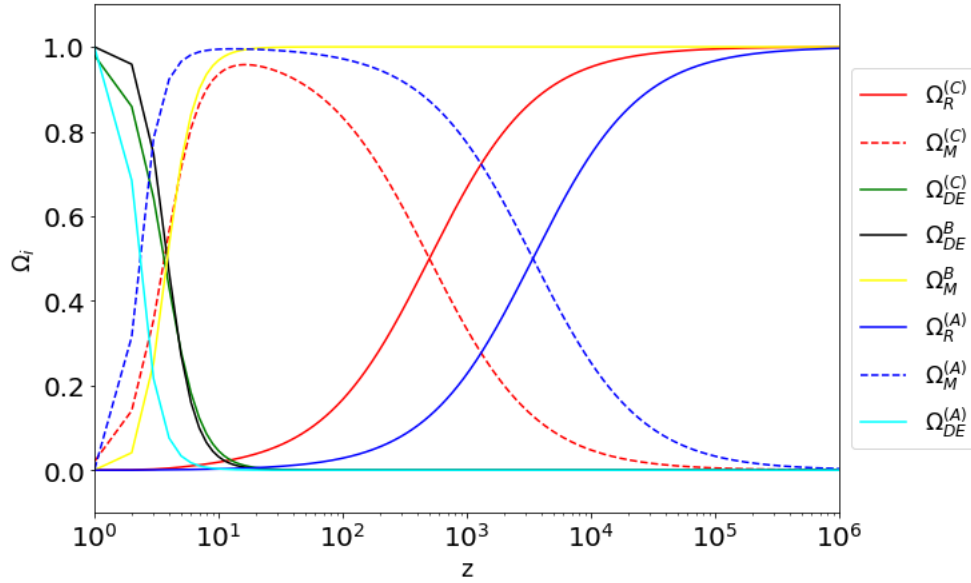


Figure 10: Evolution of energy densities as a function of redshift

which failed to demonstrate the normal behaviour as according to the standard model. These models started their cosmological evolution from the matter dominated epoch and ended at the dark energy dominated epoch, which are not the cosmologically acceptable paths. The possible cause and commonality around these models is their linearity, and the inability to show the radiation epoch in the early times of the universe. From the first models mentioned before, those with acceptable cosmological paths (**C**, **D**, **F**, **G**, and **I**), we also saw from figure 11 that radiation and matter dominated eras were decelerating ($q > 0$) while the DE epoch was accelerating ($q < 0$).

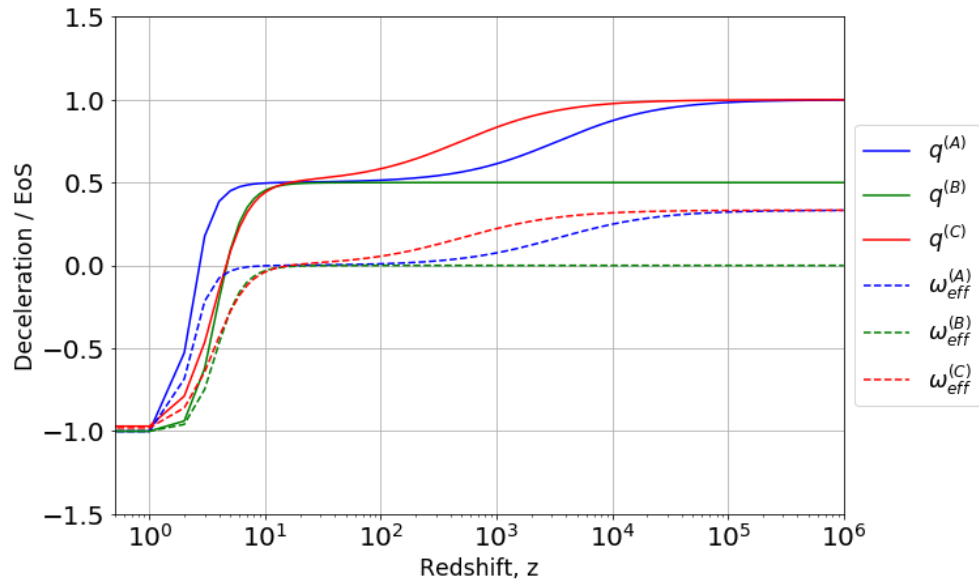


Figure 11: Evolution of deceleration parameter and EoS are plotted as a function of redshift, for the different interactions.

5 Interactions in the dark: constraints

In the last decade, cosmological data from various observations has been quickly updating, not only in terms of quantity but also in terms of quality. This allows for more trustworthy scientific discoveries and stricter limits on theoretical models in cosmology. The most recent Planck results [12] provide significant contributions to a number of theoretical cosmological investigations and have reduced more uncertainties than the older results. In this chapter we will use this newer and more precise cosmological data to aid and analyse the DM and DE interaction models.

5.1 Theoretical constraints

5.1.1 End of the radiation dominated epoch

When the radiation dominated epoch ended, and its density ρ_r was dropping as per 2.41, the matter epoch began to dominate where its density ρ_m fell off at a much lesser rate 2.46, which resulted in a point of equality where the two densities were equal. At the point where the two densities matched, we had;

$$\rho_r(t) = \rho_{0,r} \frac{a_0^4}{a^4(t)} = \rho_{0,m} \frac{a_0^3}{a^3(t)} = \rho_m(t), \quad (5.1)$$

that is,

$$\frac{a(t)}{a_0} = \frac{\rho_{0,r}}{\rho_{0,m}} = \frac{\Omega_{0,r}}{\Omega_{0,m}} = 2.93 \times 10^{-4}, \quad (5.2)$$

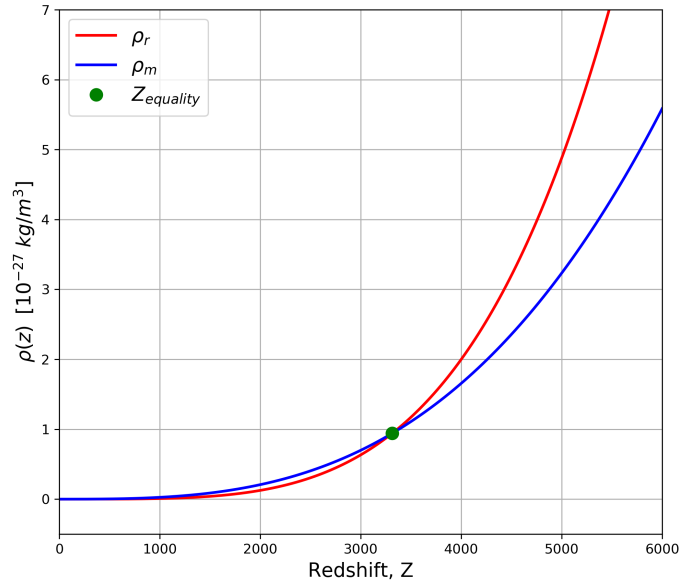
where the corresponding redshift was,

$$z = \frac{a_0}{a(t)} - 1 = 3408.27. \quad (5.3)$$

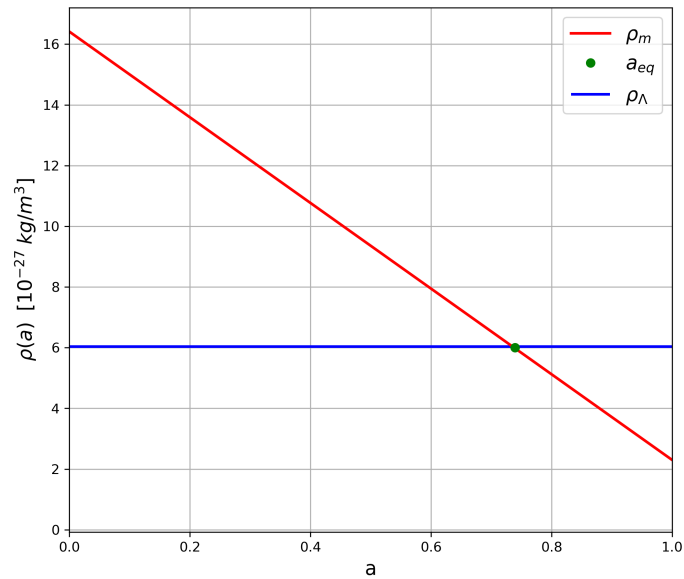
Using (2.97) we find the time at which the radiation era ended,

$$t(a = 2.93 \times 10^{-4}) = 50953 \text{ years.}$$

On figure 12a we show the point of intersection, or z_{eq} , where matter then began to dominate.



(a) Radiation and matter densities versus redshift.



(b) Matter and dark energy densities versus scale factor.

Figure 12: Plots (a) and (b) showing the equality points for radiation-matter and matter-dark energy, respectively.

5.1.2 End of the matter dominated epoch

At the end of matter dominated era, as the density was falling as per 2.46, the dark energy epoch started to dominate and the matter-dark energy densities matched at a point where

$$\rho_m(t) = \rho_{0,m} \frac{a_0^3}{a^3(t)} = \rho_{0,\Lambda}, \quad (5.4)$$

that is,

$$\frac{a(t)}{a_0} = \left(\frac{\rho_{0,m}}{\rho_{0,\Lambda}} \right)^{1/3} = \left(\frac{\Omega_{0,m}}{\Omega_{0,\Lambda}} \right)^{1/3} = 0.76458 \pm 0.01681, \quad (5.5)$$

with the corresponding redshift being,

$$z = \frac{a_0}{a(t)} - 1 = 0.31, \quad (5.6)$$

and the time at which this era ended, using (2.97), we found,

$$t(a = 0.7646) = 10.19 \text{ Gyrs.}$$

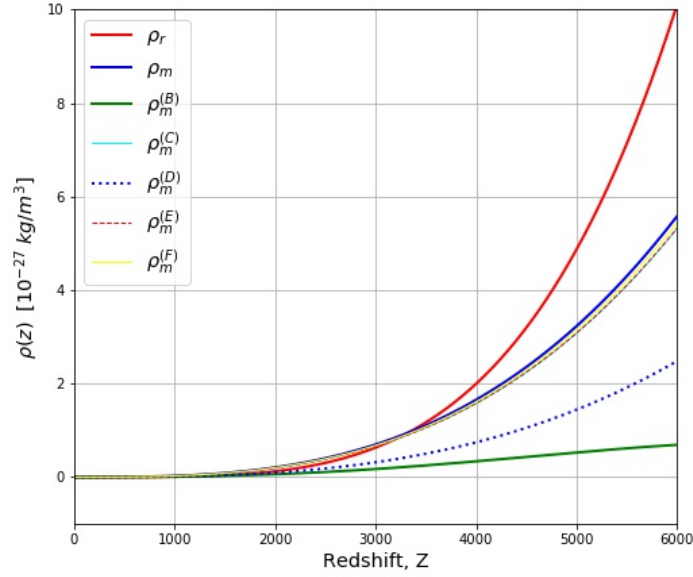
Due to the matter-dark energy equality redshift being small values and not being visible enough on a density versus redshift plot, we convert to scale factor where the corresponding value is represented on the density versus scale factor graph, as shown by figure 12b. Since the radiation density Ω_r is sub-dominant at the late times for the spatially flat universe ($\Omega_m \approx 1 - \Omega_\Lambda$), we will only look at the matter-dark energy equalities in the next sub-section.

5.1.3 End of the matter dominated epoch for different Qs

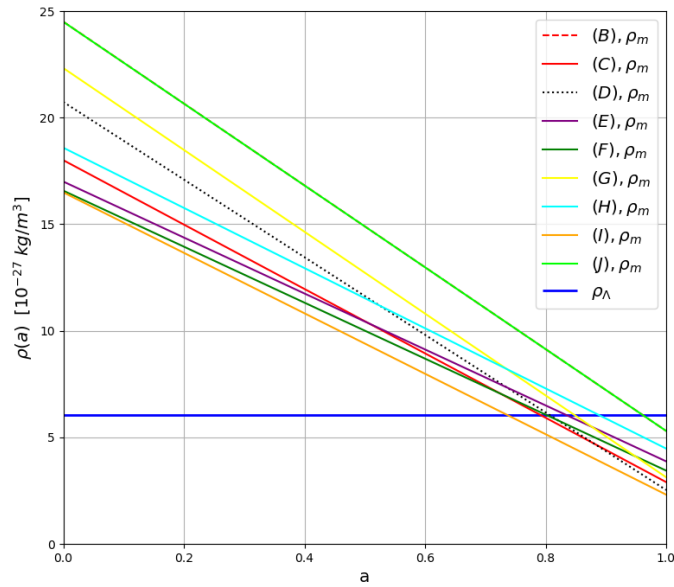
Our models showed multiple (and mostly different) redshifts of equality, or when the densities of the matter and dark-energy dominated era matched (mathematically by equation 5.4, and so on this section we interpret these redshifts for the studied models, and the times at which the equality occurred. The results are shown on Table 2. Figures 13a and 13b, shows graphically the end (intersects) of the radiation and matter epochs, respectively.

The relative expansion of the universe appears to have been delayed for most of the models, due to their forms of the interaction term as their scale factors at equality is a bit larger, that is $a_{\text{eq}} > 0.76$, as compared to the result from the Planck data equation 5.5 [12]. There is however a model (model I), where the scale factor at equality occurs as early as 9.79 Gyrs when compared to the Planck value of 10.19 Gyrs. This model has been studied further in [36].

In order to ensure stability conditions on the investigated models, we put constraints on the coupling parameter b and the results are presented on Table 3. For



(a)



(b)

Figure 13: (a) shows the radiation and matter densities as function of redshift for various Q_s , while (b) shows the matter and dark energy densities as function of scale factor.

Table 2: In this table we show the equality scale-factor with its corresponding equality redshift and the time at which the equality occurred, for the different models studied using initials 2.98.

Model	Q	a_{eq}	z_{eq}	Time (Gyr)
B	$3b^2 H \rho_{\text{tot}}$	0.96	0.04	13.20
C	$3b^2 H \rho_{\Lambda} \rho_{\text{m}} / \rho_{\text{tot}}$	0.79	0.27	10.59
D	$3b^2 H \rho_{\text{m}}^2 / \rho_{\text{tot}}$	0.80	0.25	10.75
E	$3b^2 H \rho_{\Lambda}^2 / \rho_{\text{tot}}$	0.83	0.20	11.22
F	$3b^2 H \rho_{\Lambda}^3 / \rho_{\text{tot}}^2$	0.80	0.25	10.75
G	$3b^2 H \rho_{\text{m}}$	0.85	0.18	11.53
H	$3b^2 H \rho_{\Lambda}$	0.89	0.12	12.15
I	$\eta \rho_{\text{m}}$	0.74	0.35	9.79
J	$3b^2 H (\rho_{\Lambda} + \rho_{\text{m}})$	0.96	0.04	13.20

precision cosmology, the general strategy in investigating dark energy properties is to presume that there exist a fundamental equation of state, $p_i = w_i \rho_i$, such that the field i is described, which is believed to be responsible for the universe's accelerated expansion. [37]. If the EoS falls in the interval $-1 < w_i < -1/3$, then the field i is referred to as standard quintessence, but if $w_i < -1$, then it is "phantom" since this likelihood is said to be non-canonical in Quantum Field Theory, that is, it imposes a negative kinetic energy, and also breaks the weak energy condition⁷. We can see that models **H** and **I** mimic the phantom behaviour as they both have an EoS for DE that is less than negative one. It has been shown that such models with $w < -1$, although unstable, may be constructed and might be phenomenologically realistic if seen as effective field theories that are valid only up to a specific momentum cut-off [38]. The Dominant Energy Condition (DEC) implies that $w \geq -1$ and since for cosmological reasons we are looking for a source with $\rho > 0$, we can see on Table 3 that models **B** through **G** correspond with this condition.

⁷The weak energy condition stipulates that for all time-like vector fields, the observed matter density by the corresponding observers is always non-negative.

Table 3: In this table we present the different models that were investigated, with constraints on b^2 and DE EoS.

Model	Q	Constraints	EoS for DE
B	$3b^2 H \rho_{\text{tot}}$	$b^2 < 1$	$-1 < w_{\text{eff}} < 0$
C	$3b^2 H \rho_{\Lambda} \rho_m / \rho_{\text{tot}}$	$b < 1$	$-1 < w_{\text{eff}} < -1/3$
D	$3b^2 H \rho_m^2 / \rho_{\text{tot}}$	$b^2 < 1/3(1 - m^2)$	$-1 < w_{\text{eff}} < -1/3$
E	$3b^2 H \rho_{\Lambda}^2 / \rho_{\text{tot}}$	$b^2 < (1 - m^2) / m^2$	$-1 < w_{\text{eff}} < 0$
F	$3b^2 H \rho_{\Lambda}^3 / \rho_{\text{tot}}^2$	$b^2 < (1 - m^2) / m^3$	$-1 < w_{\text{eff}} < 0$
G	$3b^2 H \rho_m$	$b^2 < 8/9$	$-1 < w_{\text{eff}} < 0$
H	$3b^2 H \rho_{\Lambda}$	$b^2 < 1$	$w_{\text{eff}} < -1$
I	$\eta \rho_m$	$v < 1$	$w_{\text{eff}} < -1$
J	$3b^2 H (\rho_{\Lambda} + \rho_m)$	$b^2 < 1$	$w_{\text{eff}} < -1$

5.2 Observational constraints

In order to constrain the dark energy equation of state, a combination of datasets from different cosmic microwave background (CMB) experiments have been studied in [3, 4] to show the constraints on EoS for DE, at certain confidence levels. Thus in this context, we will use such results and others to analyse and compare with our theoretical findings, in order to draw some conclusions. The result that EoS for DE may be less than -1 is not completely ruled out at present by cosmological data as it seems, to some degree, is preferred by the joint analysis of the supernovae (SN) and CMB data [37].

In Table 4 we see different combinations of datasets from CMB, Hubble Space Telescope (HST), Big Bang Nucleosynthesis (BBN), supernovae type Ia (SN-Ia) and finally also data from the 2dF survey [3]. The SN-Ia data enables cosmological parameters to be determined by investigating the current values of the deceleration parameter q_0 and the Hubble constant H_0 [39]. It is evident on this table that, the more combinations of datasets we use, the slimmer the constraint values of the EoS of the DE component and thus the better the result. This trend is also similar in constraining the matter density Ω_m . With more recent data as in [4], we see an improvement on the constraint of w_{eff} , shown on Table 5. It is apparent from the table results that the individual datasets constrain the DE w_{eff} very poorly and these limits are improved when combining the datasets.

Table 4: Constraint results on the equation of state for dark energy and matter density, $\Omega_m = 1 - \Omega_\Lambda$, from different combinations of datasets. The 2σ limits are obtained from integrals of 2.5% and 97.5% of the marginalized probability. [3].

Datasets	EoS for DE	Constraint on Ω_m
CMB + HST	$-1.65 < w_{\text{eff}} < -0.54$	$0.19 < \Omega_m < 0.43$
CMB + HST + BBN	$-1.61 < w_{\text{eff}} < -0.57$	$0.20 < \Omega_m < 0.42$
CMB + HST + SN-Ia	$-1.45 < w_{\text{eff}} < -0.74$	$0.21 < \Omega_m < 0.36$
CMB + HST + SN-Ia + 2dF	$-1.38 < w_{\text{eff}} < -0.82$	$0.22 < \Omega_m < 0.35$

Table 5: Constraint results on the equation of state for dark energy and matter density, $\Omega_m = 1 - \Omega_\Lambda$ from individual and a combination of the datasets, at the 3σ confidence limit. [4].

Datasets	EoS for DE	Constraint on Ω_m
SN-Ia	$-1.57 \leq w_{\text{eff}} \leq -0.66$	$0.05 \leq \Omega_m \leq 0.43$
BAO	$-2.19 \leq w_{\text{eff}} \leq -0.42$	$0.19 \leq \Omega_m \leq 0.36$
H(z)	$-1.78 \leq w_{\text{eff}} \leq -0.72$	$0.20 \leq \Omega_m \leq 0.35$
SN-Ia + BAO + H(z)	$-1.13 \leq w_{\text{eff}} \leq -0.95$	$0.25 \leq \Omega_m \leq 0.31$

6 Discussions and conclusion

An investigation was performed, using dynamical systems, on the impacts of interactions between dark matter and dark energy on the evolution of the universe. In the first chapter of this work an introduction on the expansion of the universe was presented. With more and more accurate data generated, we saw that the Hubble constant, which is the proportionality constant in the Hubble–Lemaître law 1.1, has changed and improved over time. The current value of this constant, as presented in [12] is 67.74 ± 0.46 km/sMpc. We also introduced the dark sector components, namely, dark matter and dark energy. The cosmological constant Λ is the simplest candidate for DE. More recently, it has been discussed in [16] how the axion has emerged as a DM candidate and how it was produced in the early phases of the universe. It has been said that ever since the discovery of the universe’s current accelerating expansion in 1998, dark energy has played a significant role in cosmological studies [40].

Despite the Λ CDM model’s success in explaining the formation and evolution of large scale structure in the universe; the state of the early universe, the abundance of various forms of matter and energy; and its predictive power, according to the majority of the cosmology community, it presents several challenges [22, 41]. Among the most popular of these includes the “cosmic coincidence problem” and the “cosmological constant fine tuning problem”. In the framework of the aforementioned model, we derived Friedmann equations and solutions, considering three spatial curvatures of the universe: closed, open and flat universes. Using data from [12] we calculated the age of the universe today as 13.78 billion years.

Dynamical systems were introduced in the third chapter of this work. Since our main purpose was to provide a qualitative description of the interaction models investigated, this method came in handy. Friedmann equations were reduced to dimensionless variables, from which we then used the aforementioned technique to generalize the equations into ODEs in two dimensions. The eigenvalue combinations and explanations were presented in Table 1, which we used to aid our analyses of the stability and classification of the fixed points for each model studied.

We introduced and studied different possible interaction terms between the dark sector components in chapter four. We observed a behaviour similar to the Λ CDM model when there is no interaction, $Q = 0$, that is, where the trajectories on the phase space plot started from the unstable radiation dominated era, passed through the also unstable matter dominated epoch, and ended at the stable dark energy dominated epoch. This was a display of the acceptable cosmological paths we desired. Such behaviour was observed for multiple other models (C, D, F, G,

and I). However, there were some interaction terms (**B**, **E**, **H**, and **J**) between DM and DE that we noticed a system's break down in the early times of the universe (the system 3.26 was divergent), and so they only displayed trajectories that started from the matter dominated epoch up to the dark energy dominated epoch.

The equality redshift (and scale factor), for when there was a radiation-matter and matter-dark energy match in densities using the Planck 2018 data, was presented; from which we saw that these events occurred at redshifts $z_{\text{eq}} = 3408.27$ and $z_{\text{eq}} = 0.31$, respectively. Since we considered DM-DE interactions, we also worked out the DM-DE equality redshifts for our models and presented the results on Table 2. To ensure stability of the models studied, we placed constraints on the coupling constant b^2 which allowed us to constrain the effective EoS for dark energy. The results were presented on Table 3.

Whilst making sure we preserve the dominant energy condition and that our results are comparable to the Λ CDM model, we discovered models **C** through **G** to be in good agreement. With these models being possible candidates of the interaction term between dark sector components, however, model **C** emerged as the *best possible* candidate to helping us answer the natural question: what is the form of the interaction term between the two dark sector components? Observational tests on the studied models can make significant improvement in better constraining and providing tighter bounds on the parameters, and proving better solutions to the said question.

Acknowledgements

VM acknowledges funding through the National Astrophysics and Space Science Program (NASSP) and National Research Foundation (NRF) scholarship.

References

- [1] B. Ryden, *Introduction to cosmology*. Cambridge University Press, 2017.
- [2] University of Oregon, "Geometry of the Universe." [Online]. Available: <http://abyss.uoregon.edu/%7Ejs/cosmo/lectures/lec15.html>
- [3] A. Melchiorri *et al.*, "The state of the dark energy equation of state," *Physical Review D*, vol. 68, no. 4, p. 043509, 2003.
- [4] A. Tripathi *et al.*, "Dark energy equation of state parameter and its evolution at low redshift," *Journal of Cosmology and Astroparticle Physics*, vol. 2017, no. 06, p. 012, 2017.
- [5] A. G. Riess *et al.*, "Observational evidence from supernovae for an accelerating universe and a cosmological constant," *The Astronomical Journal*, vol. 116, no. 3, p. 1009, 1998.
- [6] S. Perlmutter *et al.*, "Measurements of Ω and Λ from 42 high-redshift supernovae," *The Astrophysical Journal*, vol. 517, no. 2, p. 565, 1999.
- [7] M. Tegmark *et al.*, "Cosmological parameters from SDSS and WMAP," *Physical review D*, vol. 69, no. 10, p. 103501, 2004.
- [8] D. N. Spergel *et al.*, "First-year Wilkinson Microwave Anisotropy Probe (WMAP)* observations: determination of cosmological parameters," *The Astrophysical Journal Supplement Series*, vol. 148, no. 1, p. 175, 2003.
- [9] S. M. Carroll, "Why is the universe accelerating?" in *AIP Conference Proceedings*, vol. 743, no. 1. American Institute of Physics, 2004, pp. 16–32.
- [10] E. P. Hubble, *106. A Relation between Distance and Radial Velocity among Extra-Galactic Nebulae*. Harvard University Press, 2013.
- [11] H. Kragh, "Hubble Law or Hubble-Lemaître Law? The IAU Resolution," *arXiv preprint arXiv:1809.02557*, 2018.
- [12] K. Cahill, "The eras of radiation, matter, and dark energy: new information from the planck collaboration," *arXiv preprint arXiv:1606.08865*, 2016.
- [13] M. Z. Iqbal *et al.*, "Progress in physics of the cosmos," *International Journal of Astronomy and Astrophysics*, vol. 5, no. 02, p. 79, 2015.

- [14] P. J. E. Peebles, "Growth of the nonbaryonic dark matter theory," *Nature astronomy*, vol. 1, no. 3, pp. 1–5, 2017.
- [15] K. J. Ludwick, "Possible couplings of dark matter," *arXiv preprint arXiv:1809.09971*, 2018.
- [16] F. Chadha-Day, J. Ellis, and D. J. Marsh, "Axion dark matter: What is it and why now?" *arXiv preprint arXiv:2105.01406*, 2021.
- [17] M. Demianski *et al.*, "Investigating dark energy equation of state with high redshift hubble diagram," *arXiv preprint arXiv:2010.05289*, 2020.
- [18] A. Riess, "Dark energy," *Encyclopædia Britannica*, 2017. [Online]. Available: <https://www.britannica.com/science/dark-energy>
- [19] M. S. Berger and H. Shojaei, "Interacting dark energy and the cosmic coincidence problem," *Physical Review D*, vol. 73, no. 8, p. 083528, 2006.
- [20] E. J. Copeland *et al.*, "Dynamics of dark energy," *International Journal of Modern Physics D*, vol. 15, no. 11, pp. 1753–1935, 2006.
- [21] M. Roos, "Expansion of the Universe-Standard Big Bang Model," Tech. Rep., 2008.
- [22] S. Weinberg, "The cosmological constant problem," *Reviews of Modern Physics*, vol. 61, no. 1, p. 1, 1989.
- [23] A. G. Riess *et al.*, "Large Magellanic Cloud Cepheid standards provide a 1% foundation for the determination of the Hubble constant and stronger evidence for physics beyond Λ CDM," *The Astrophysical Journal*, vol. 876, no. 1, p. 85, 2019.
- [24] P. Peebles, "1. The Standard Cosmological Model," in *Principles of Physical Cosmology*. Princeton University Press, 2020, pp. 3–10.
- [25] B. A. Robson *et al.*, "Introductory Chapter: Standard Model of Cosmology," in *Redefining Standard Model Cosmology*. IntechOpen, 2019.
- [26] A. De Simone *et al.*, "Introduction to cosmology and dark matter," in *CERN European School for High Energy Physics (ESHEP) 2018.*, vol. 6. CERN, 2019, pp. 145–180.
- [27] IB Revision, "Astrophysics Part V: The End of the Universe," 2013. [Online]. Available: <https://ibeconsphysics.wordpress.com/>

- [28] A. Coley, "Dynamical Systems and Cosmology," *Astrophysics and Space Science Library*, vol. 291, 2003.
- [29] C. G. Böhmer and N. Chan, "Dynamical systems in cosmology," in *Dynamical and Complex Systems*. World Scientific, 2017, pp. 121–156.
- [30] G. Layek, *An introduction to dynamical systems and chaos*. Springer, 2015.
- [31] H. Golchin *et al.*, "Interacting dark energy: Dynamical system analysis," *International Journal of Modern Physics D*, vol. 26, no. 09, p. 1750098, 2017.
- [32] R.-G. Cai *et al.*, "More on QCD ghost dark energy," *Physical Review D*, vol. 86, no. 2, p. 023511, 2012.
- [33] R. Garcia-Salcedo *et al.*, "Phase Space Dynamics of Non-Gravitational Interactions between Dark Matter and Dark Energy: The Case of Ghost Dark Energy," *arXiv preprint arXiv:1211.2738*, 2012.
- [34] W. Yang *et al.*, "Tale of stable interacting dark energy, observational signatures, and the H_0 tension," *Journal of Cosmology and Astroparticle Physics*, vol. 2018, no. 09, p. 019, 2018.
- [35] W. Yang, S. Pan, E. Di Valentino, O. Mena, and A. Melchiorri, "2021- H_0 Odyssey: Closed, Phantom and Interacting Dark Energy Cosmologies," *arXiv preprint arXiv:2101.03129*, 2021.
- [36] S. K. Biswas *et al.*, "Dynamical analysis of an interacting dark energy model in the framework of a particle creation mechanism," *Physical Review D*, vol. 95, no. 10, p. 103009, 2017.
- [37] J. Solà and H. Štefančić, "Effective equation of state for dark energy: Mimicking quintessence and phantom energy through a variable Λ ," *Physics Letters B*, vol. 624, no. 3-4, pp. 147–157, 2005.
- [38] S. M. Carroll *et al.*, "Can the dark energy equation-of-state parameter w be less than -1?" *Physical Review D*, vol. 68, no. 2, p. 023509, 2003.
- [39] S. Capozziello, "Curvature quintessence," *International Journal of Modern Physics D*, vol. 11, no. 04, pp. 483–491, 2002.
- [40] L. G. Collodel and G. M. Kremer, "Non-minimally coupled tachyon field with Noether symmetry under the Palatini approach," in *AIP Conference Proceedings*, vol. 1647, no. 1. American Institute of Physics, 2015, pp. 29–34.
- [41] A. Del Popolo and M. Le Delliou, "Small scale problems of the Λ CDM model: a short review," *Galaxies*, vol. 5, no. 1, p. 17, 2017.